UNIVERSIDADE ESTADUAL PAULISTA
"JULIO DE MESQUITA FILHO"
INSTITUTO DE GEOCIÊNCIAS E CIÊNCIAS EXATAS

Dissertação de Mestrado

Programa de Pós-Graduação em Geografia

VEGETATION MULTITEMPORAL RESPONSES TO HYDROCLIMATE VARIATIONS IN THE ESPINHAÇO RANGE (BRAZIL)

João Francisco Ferreira Sobreiro

Prof. Dr. Thiago Sanna Freire Silva (orientador)

Rio Claro (SP)

2019

UNIVERSIDADE ESTADUAL PAULISTA

“Júlio de Mesquita Filho”

Instituto de Geociências e Ciências Exatas

Câmpus de Rio Claro

JOÃO FRANCISCO FERREIRA SOBREIRO

VEGETATION MULTITEMPORAL RESPONSES TO HYDROCLIMATE VARIATIONS IN THE ESPINHAÇO RANGE (BRAZIL)

Dissertação de Mestrado apresentada ao Instituto de Geociências e Ciências Exatas do Câmpus de Rio Claro, da Universidade Estadual Paulista “Júlio de Mesquita Filho”, como parte dos requisitos para obtenção do título de Mestre em Geografia.

Orientador: Prof. Dr. Thiago Sanna Freire Silva

Rio Claro - SP

2019

UNIVERSIDADE ESTADUAL PAULISTA

S677v

Sobreiro, João Francisco Ferreira
Vegetation multitemporal responses to hydroclimate variations in the Espinhaço Range (Brazil) / João Francisco Ferreira Sobreiro. -- Rio Claro, 2019
73 p. : il., tabs., mapas + 1 CD-ROM

Dissertação (mestrado) - Universidade Estadual Paulista (Unesp), Instituto de Geociências e Ciências Exatas, Rio Claro
Orientador: Thiago Sanna Freire Silva

1. Hidroclimatologia. 2. Sensoriamento Remoto. 3. Montanha. 4. Espinhaço. 5. Vegetação. I. Título.

Sistema de geração automática de fichas catalográficas da Unesp. Biblioteca do Instituto de Geociências e Ciências Exatas, Rio Claro. Dados fornecidos pelo autor(a).

Essa ficha não pode ser modificada.

“Júlio de Mesquita Filho”

Instituto de Geociências e Ciências Exatas

Câmpus de Rio Claro

JOÃO FRANCISCO FERREIRA SOBREIRO

VEGETATION MULTITEMPORAL RESPONSES TO HYDROCLIMATE VARIATIONS IN THE ESPINHAÇO RANGE (BRAZIL)

Dissertação de Mestrado apresentada ao Instituto de Geociências e Ciências Exatas do Câmpus de Rio Claro, da Universidade Estadual Paulista “Júlio de Mesquita Filho”, como parte dos requisitos para obtenção do título de Mestre em Geografia.

Comissão Examinadora

Prof. Dr. Thiago Sanna Freire Silva (Orientador)

Prof. Dr. Humberto Ribeiro da Rocha

Dra. Bruna de Costa Alberton

Conceito: APROVADO

Rio Claro/SP, 11 de junho de 2019

Rio Claro - SP

2019

AGRADECIMENTOS

- O presente trabalho foi realizado com apoio da Coordenação de Aperfeiçoamento de Pessoal de Nível Superior – Brasil (CAPES) – Código de Financiamento 001;

- Agradecimento à Fundação de Amparo à Pesquisa do Estado de São Paulo (FAPESP #2013/50155-0 - FAPESP-Microsoft Reasearch Institute) pelo apoio ao projeto.

RESUMO

Os sistemas montanhosos são laboratórios naturais para análise de gradientes. Elevação, amplitude e diferenças topográficas em montanhas podem criar fortes diferenças microclimáticas a curtas distâncias, aninhadas dentro da mesma região biogeográfica e macroclimática, permitindo-nos compreender melhor as respostas da vegetação e os feedbacks sobre a disponibilidade de água. Neste estudo, avaliamos como a distribuição da vegetação está ligada à disponibilidade de água na Serra do Espinhaço. Para tanto, abordamos as seguintes questões: 1) Quais são os regimes hidroclimáticos encontrados na Serra do Espinhaço e seus correspondentes tipos de vegetação? 2) Onde a produtividade da vegetação é mais e / ou menos acoplada aos regimes hidroclimáticos? 3) A topografia é capaz de impactar a produtividade da vegetação e suas relações de acoplamento com regimes hidroclimáticos? Além disso, considerando estas relações ambientais e de vegetação, 4) Como a resiliência climática dos tipos de vegetação nesta região varia? Conclui-se que na faixa do Espinhaço, a maior parte da dinâmica de produtividade da vegetação espaço-temporal é impulsionada por condições hidroclimáticas e / ou topo-edáficas. Nossos resultados mostram que a vegetação da Caatinga teve uma resposta plástica e relativamente rápida ao Déficit Hídrico Climático (CWD) e foi o tipo de vegetação com maior restrição hídrica. Cerrado e Campos Rupestres tiveram respostas semelhantes às flutuações no déficit hídrico, mostrando um gradiente de respostas das mais lentas as mais rápidas entre regiões hidroclimáticas “Humid” a “Very Dry”. A Mata Atlântica não apresentou um padrão claro de resposta à sazonalidade na disponibilidade de água. Também descobrimos que entre todos os biomas analisados, o Cerrado e a Mata Atlântica foram os mais sensíveis em relação à variabilidade interanual do CWD, especialmente em locais com condições úmidas. Desde que, no período avaliado, essas regiões não apresentaram alta variabilidade de CWD ano a ano, argumentamos que anos climáticos mais extremos podem ter um grande impacto na capacidade dessas fenologias de vegetação rastrearem a variabilidade interanual.

PALAVRAS-CHAVE

Hidroclimatologia; Sensoriamento Remoto; Montanha; Vegetação; Espinhaço

ABSTRACT

Montane systems are natural laboratories for gradient analysis. Elevation, amplitude and topographical differences over mountains can create strong microclimatic differences over short distances, nested within the same biogeographic and macro-climatic region, thus allowing us to better understand vegetation responses and feedbacks to water availability. In this study, we assessed how vegetation distribution is linked to water availability in the Espinhaço Mountain Range. For that, we addressed the following questions: 1) Which are the hydroclimatic regimes found in the Espinhaço Range and their corresponding vegetation types? 2) Where does vegetation productivity is more and/or less coupled to hydroclimatic regimes? 3) Is topography able to impact vegetation productivity and its coupling relations to hydroclimatic regimes? Also, considering these environmental and vegetation relationships, 4) How does the climatic resilience of the vegetation types in this region vary? We conclude that in the Espinhaço Range, most of the spatio-temporal vegetation productivity dynamics are driven by hydroclimatic and/or topo-edaphic conditions. Our results show that "*Caatinga*" vegetation had a plastic and relatively fast response to Climatic Water Deficit (CWD) and was the most water-constrained vegetation type. "*Cerrado*" and "*Campos Rupestres*" had similar responses to fluctuations in water deficit, showing a gradient of slower to faster responses from "*Humid"* to "*Very dry*" hydroclimatic regions. "*Mata Atlântica*" did not show a clear pattern of responses to seasonality on water availability. We also found that among all biomes analyzed, "*Cerrado*" and "*Mata Atlântica*" was the most sensitive regarding the CWD interannual variability, especially in sites with moist conditions. Since over the period assessed those regions did not presented high variability on year-to-year CWD, we argue that more extreme climatic years can have a large impact on the capacity of these vegetation phenology tracking interannual variability.

KEYWORDS

Hydroclimatology; Remote Sensing; Mountain; Vegetation; Espinhaço

Summary

1. INTRODUCTION

The distribution, structure and functioning of terrestrial ecosystems are fundamentally climate controlled. Temperature and water availability, for example, drive the rates at which chemical and biological reactions can occur (Bonan, 2016). Climate system components are modulators of ecosystem dynamics, but are also influenced by biological processes and feedbacks, such as vegetation shading and evapotranspiration rates (Oliveira *et al.*, 2014). Therefore, a good understanding of spatial and temporal variations in climate is critical to better assess and predict ecosystem processes and functioning.

In the tropics, vast areas experience seasonally dry climates, with a well-defined wet season during which most of the annual precipitation occurs, followed by a prolonged dry season (Vico *et al.*, 2015). These areas usually harbor a gradient of vegetation functional types, from moist to dry forests (Vico *et al.*, 2015; Allen *et al.*, 2017). In seasonally dry environments, climatic influences on ecosystem function have been shown to have greater impact when compared to less seasonal regions (Allen *et al.*, 2017). This is a result of the inter-seasonal temporal fluctuations of resource availability, which drive major ecosystem processes such as vegetation phenology (Bencke and Morellato, 2002; Chambers *et al.*, 2013; Streher *et al.*, 2017).

Tropical dry vegetation phenology is known to be coupled with inter and intra-annual differences in rainfall, and therefore water availability (Fenner, 1998). Nevertheless, local and regional studies of tropical seasonally-dry ecosystems show that plant leafing phenology can be more correlated to photoperiod and temperature than to precipitation (de Camargo *et al.*, 2018). These differences emphasize the high complexity of these ecosystems and the feedbacks between them and environmental resources. One way to address this complexity is thus by

analyzing differential vegetation distribution over environmental gradients, such as mountainous regions (Graham *et al.*, 2014).

Mountainous ecosystems are recognized for the uniqueness of their ecological processes, as topography-driven isolation increases speciation rates and promotes high levels of species richness and endemism (Steinbauer *et al.*, 2016). These processes are a result of the different microclimatic zones confined across elevational gradients over short geographical distances (Pepin *et al.*, 2015). Despite recent observations of higher warming rates in tropical mountains, we still need to improve our understanding of how topo-climatic drivers influence vegetation distribution over montane regions, and therefore predict biodiversity responses under different climate change scenarios (Rangwala and Miller, 2012; Krishnaswamy, John and Joseph, 2014).

Montane systems are natural laboratories for gradient analysis. Elevation, amplitude and topographical differences over mountains can create strong microclimatic differences over short distances, nested within the same biogeographic and macro-climatic region, thus allowing us to better understand vegetation responses and feedbacks to water availability, temperature amplitude, photoperiod exposure, and soil biological and physical dynamics, minimizing the regional variation of climate seasonality (Aparecido *et al.*, 2018). Furthermore, montane ecosystems are specially threatened by climate change, as species will seek colder temperatures over elevational gradients, thus increasing competition with high-elevation adapted plants (Rangwala and Miller, 2012; Pepin *et al.*, 2015).

Seasonally dry tropical environments are expected to experience future changes in periodicity due to climate change, with stronger impacts predicted for higher elevations (Kohler and Maselli, 2012; Elsen and Tingley, 2015; Pepin *et al.*, 2015; Aparecido *et al.*, 2018). Among other impacts, tropical montane ecosystems will potentially suffer an acceleration of their

hydrological regimes, caused by an increase on the variability of precipitation patterns (Allan and Soden, 2008), leading to, among others, changes in ecosystem functioning and productivity, increasing mortality rates, and/or shifting environmental conditions towards states that are more favorable to invasive species, therefore impacting species diversity and distribution. For this reason, understanding and quantifying the spatial and temporal patterns of water use strategies from seasonal vegetation can provide important insights on how tropical mountainous ecosystems will respond to climate change.

Given the above, we present here a study of the bioclimatic and ecohydrological relations of climate-vegetation systems in a tropical montane system spanning a gradient from seasonally dry to humid regions in Brazil. The Espinhaço Range is a mountainous region feeding the watersheds of two large river basins with an S-N direction in Brazil's interior. This region is an ecotone of semi-deciduous moist forests, savannas, dry forests and mountain vegetation. This ancient landscape, dating back to 640 Mya, has large topographic and altitudinal variation, with mountain peaks reaching over 2000 meters *a.s.l* (Schaefer *et al.*, 2016).

A recent analysis of spatial precipitation patterns in the Espinhaço Range showed that there is no significant difference in total annual rainfall between the eastern and western sides of the range, which are mainly covered by semi-deciduous moist forest and savanna vegetation, respectively (Streher *et al.*, 2017). Previous studies have shown evidence of local orographic effects on rainfall patterns (Rapini *et al.*, 2008; Ribeiro *et al.*, 2009; Santos, Serafim and Sano, 2011), but this difference in precipitation does not hold at broader scales, suggesting that more complex climatic controls (precipitation seasonality; water availability; evaporative demand) and feedbacks (nutrient availability; fire activity) are likely responsible for the distribution of different vegetation types along the range.

To understand the relations between vegetation distribution and water use strategy in this tropical vegetation mosaic over a topographically complex bioclimatic ecotone, we used remotely sensed data of vegetation structure, productivity, and evapotranspiration to assess the length and magnitude of vegetation responses to drought in the Espinhaço Mountain Range, under the water and energy conservation theoretical framework. Specifically, we addressed the following questions:

1) Which are the hydroclimatic regimes found in the Espinhaço Range and their corresponding vegetation types?

2) Where does vegetation productivity is more and/or less coupled to hydroclimatic regimes?

3) Is topography able to impact vegetation productivity and its coupling relations to hydroclimatic regimes? Also, considering these environmental and vegetation relationships,

4) How does the climatic resilience of the vegetation types in this region vary?

2. THEORETICAL BACKGROUND

2.1 Conceptual basis

Water availability is a main driver of terrestrial ecosystem function and variability. Water availability to plants is most closely given by soil moisture, which is the direct link between precipitation and ecological systems (Weltzin et al. 2003). Soil moisture is a function of water inputs and outputs of a given land surface, including processes such as precipitation interception by plants, water infiltration and runoff. The physical basis of tthese processes is relatively well understood, but quantifying and modelling then over space and time, and therefore measuring soil moisture remains a challenge (Schwinning *et al.*, 2004; Fekete, Pisacane and Wisser, 2016).

Soil moisture is a component of the total amount of water held in a soil profile, known as soil water. Soil water can be divided into four zones; root zone, intermediate zone, capillary fringe and groundwater (Figure 1). The rooting zone, where plants typically have most of their roots, accounts for the greatest portion of the water available to vegetation of an ecosystem, since vegetation extracts water from this soil layer to replenish water lost through transpiration. This zone has large variability in water content and is highly dependent on topography, precipitation intensity and temperature amplitude, as it is often saturated during heavy rainfall events but quickly becomes unsaturated as a result of water drained downward due to gravity force (percolation) and evaporative processes (Bonan, 2016).

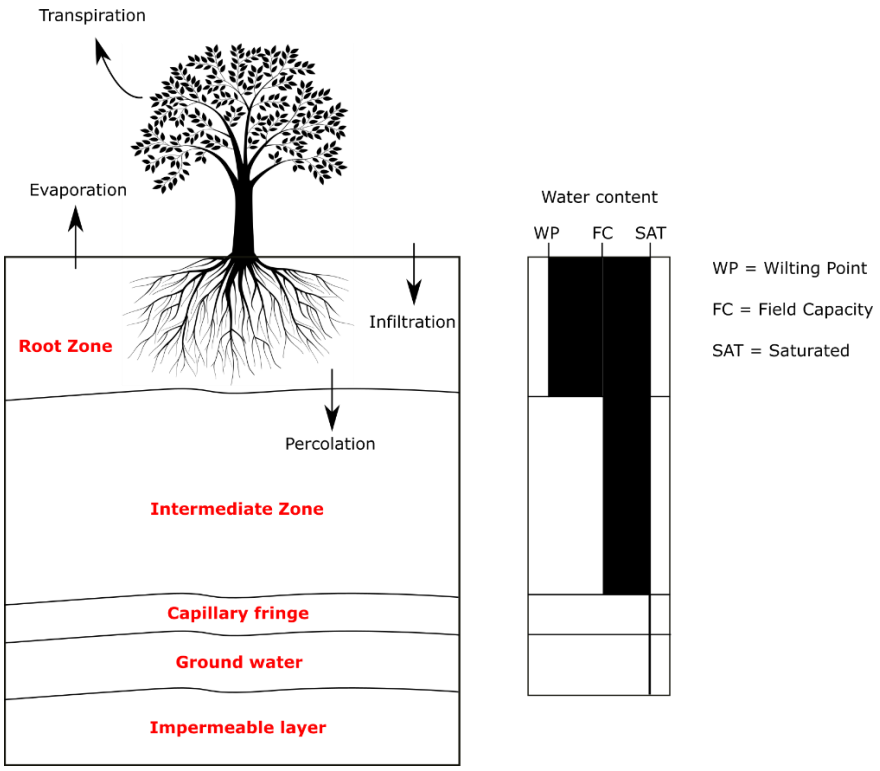

Figure 1: Typical soil water zones and movements, modified from Bonan, 2016. (Bonan, 2016).

An important mechanism of soil water movement is known as hydraulic lift, which is water redistribution within the soil profile made by plant roots (Bonan, 2016). This process allows a drier upper soil layer to receive water from wetter deeper layers, and has been widely shown in the literature to be an important phenomenon on water use strategies at arid to semi-arid environments (Meinzer *et al.*, 2004; Domec *et al.*, 2010; Neumann and Cardon, 2012).

Variations in soil moisture or water availability to plants is a result of the water cycle, a complex system that can be simplified, for this purpose, into an equation where soil water changes are the balance between water input from precipitation, water loss from evapotranspiration, and water lost as runoff (Equation 1):

$$\textbf{(Eq. 1)}\ \Delta S = P - E - R$$

Where, ΔS is change in soil water, P is precipitation, E is evapotranspiration and R is runoff.

Direct observations of soil moisture are expensive, time consuming and point-based, and usually do not represent the high spatial and temporal variability of water soil dynamics, and therefore inadequate to carry out regional and global studies (LIU *et al.*, 2009). However, recently technological advances have allowed the development of satellite remote sensed methods to improve the estimation of soil moisture at large spatial scales, such as satellite derived measurements and modelling of evapotranspiration, a major proxy of soil moisture.

2.2 Transpiration and Evaporation

The cycling of water over land is controlled by the availability of solar energy, which favors the evaporation of water from soils, lakes, rivers and oceans and/or the condensation of water vapor into clouds, and eventually precipitation. These processes drive the balance between water inputs and outputs in ecosystems function, essential to maintain plant growth and development (McLaughlin *et al.*, 2017).

Water reaches the surface by precipitation, in the form of rainfall or snow, and will be available to plants depending on its intensity, frequency and duration, since this timing will affect how and if water will penetrate in the soil upper layers. The leaf area index of a given land surface will also impact water availability, since a dense canopy intercepts more water than a leafless one. The interception capacity and amount of water held in the canopy has a significant effect on climate because it readily evaporates (Davies-Barnard et. Al, 2014).

Evaporation results from a moist surface which is exposed to drier air, being that as air parcels move away from the surface, they carry with them the evaporated moisture (Bonan, 2016). Evaporation is limited by the amount of water vapor in the surrounding air, and when the air is saturated with water vapor, evaporation ceases. Transpiration is evaporation of water from plants as it moves from the soil through plants and out through the leaves to the free air. Plant

transpiration is also regulated by the physiology of plants, being greater in areas with higher surface plant cover, and lower in surfaces with low plant cover, where evaporation becomes the dominant flux (Frank *et al.*, 2015). Since it is difficult to separately measure evaporation from transpiration, the two terms are often combined into evapotranspiration.

Evapotranspiration is expressed as the rate of evaporated water of a given land surface area over a specific time period, and it depends directly on the availability of energy to evaporate water and the ability of water vapor to diffuse into the atmosphere. In this way, tropical climates, which receives high amounts of energy, have greater capacity to evaporate water than arctic climates, for example (Nathan L. Stephenson, 1990). Besides this latitudinal effect, within the same latitude evapotranspiration rates will vary according to air humidity and wind speed. Dry air has a greater evaporative demand than humid air. Under calm conditions (slow wind speeds) evapotranspiration decreases as the air becomes water saturated, while under windy conditions, saturated air parcels move away and are replaced by drier ones (Aparecido *et al.*, 2018).

In addition to the atmospheric conditions controlling evapotranspiration rates, the type of soil and its water content also regulate it, as evapotranspiration rates are determined by the rate at which water is supplied to the surface. Different types of soils have different capacities of retaining and distributing water, also known as hydraulic conductivity (Volaire, 2018). Since evapotranspiration will extract water from the soil upper layers, a dry soil or a soil with low hydraulic conductivity provides less water for evapotranspiration than does a wet soil or one with high hydraulic conductivity.

The type of vegetation is also essential when analyzing and measuring evapotranspiration. Plant growth is conditioned to its capacity to absorb CO_2 through the opening of stomata during

photosynthesis (Bonan, 2016). When the stomata are open, water inside the leaf diffuses out to the surrounding drier air during transpiration, being that if too much water is lost the plant becomes desiccated and will depend on the soil water availability (Stephenson, 1998). Because of that, plants have evolved different strategies to balance its growth and cope with possible situations of water stress. Given these strategies, disentangling the rates of evapotranspiration over different ecosystems help us assess vegetation capacities to allocate carbon under favorable conditions, and to better understand how it behaves under stressful conditions, such as extremely dry years.

Finally, evapotranspiration is divided into two different forms, Potential Evapotranspiration and Actual Evapotranspiration. Potential Evapotranspiration, hereafter PET, is related to the capacity of the atmosphere to remove water from the land surface, while Actual Evapotranspiration, hereafter AET, defines the amount of water that is actually evaporated, which is limited to the maximum value of PET. PET and AET are estimated by several different models.

In this study we used the TerraClimate dataset (Abatzoglou *et al.*, 2018) to infer PET and AET values, and therefore the Climatic Water Deficit (CWD), which is the difference between PET and AET. TerraClimate products, which are gridded (~ 4km) monthly data climatic products from 1958 to 2017, are generated from the interpolation of different global weather station databases from WorldClim (version 1.4 and version 2.0), CRU Ts4.0 and JRA-55.

Potential Evapotranspiration (PET) in this dataset is calculated using the Penman-Montieth approach, where the latent heat flux (λ ET) represents the evapotranspiration fraction) (Allen *et al.*, 1998) (Equation 2).

$$\textbf{(Eq. 2)}\ \lambda ET = \Delta(R_n - G) + p_a c_p$$

where R_n is the net radiation, G is the soil heat flux, (e_s - e_a) represents the vapor pressure deficit of the air, p_a is the mean air density at constant pressure, c_p is the specific heat of the air, Δ represents the slope of the saturation vapor pressure temperature relationship, γ is the psychrometric constant, and r_s and r_a are the (bulk) surface and aerodynamic resistances.

To calculate AET and CWD, TerraClimate uses a one-dimensional modified Thornthwaite-Mather (1955) climatic water-balance model (WBM) (Lutz, van Wagtendonk and Franklin, 2010) which incorporates soil water-holding capacity, slope and aspect, with CWD given as the difference between PET and AET.

The WBM is a single bucket model applied consistently across global land surfaces that operates on a monthly time step and considers the interplay between precipitation, PET, as well as soil and snowpack water storage. The WBM accounting scheme considers runoff as the excess of liquid water supply (precipitation and snowmelt) used by monthly PET and soil moisture recharge. Soil water is extracted by the atmosphere during months where PET exceeds liquid water supply, with the extraction efficiency of soil water declining exponentially with the ratio of soil water to extractable soil water capacity. Under such conditions, AET is counted as the liquid water supply plus the soil water utilized.

Since the model requires data on plant extractable soil water capacity, it incorporates the extractable soil water storage gridded data from Wang-Erlandsson *et. al* (Wang-Erlandsson *et al.*, 2016), with a lower bound on plant extractable soil water of 10mm and a default value of 50mm for places lacking data. TerraClimate is freely available at http://climatologylab.org/terraclimate.html.

2.3 Vegetation productivity and biomass allocation as a function of climate and their estimations

Tropical ecosystems, including forests, savannas and grasslands together account for more than one-half of the world's annual carbon uptake by terrestrial vegetation. This is possible by the bioclimatic conditions found in their occupied latitudes, where temperature, precipitation and evapotranspiration regulate net primary production. Since evapotranspiration is calculated as a function of precipitation and temperature, it provides a good relationship with plant production. For example, sites with low annual evapotranspiration have low productivity, resulting from either low temperatures, limited water availability, or both (Hawkins *et al.*, 2003).

Monitoring global vegetation productivity has been possible by satellite-derived measures of plant physiological activity such as the normalized difference vegetation index (NDVI). NDVI is a measurement of the difference in electromagnetic radiation reflectance between the visible and near-infrared spectral regions (Equation 3):

$$\textbf{(Eq. 3)}\ \mathrm{NDVI} = (r_{nir} - r_{red}) / (r_{nir} + r_{red})$$

where r_{nir} and r_{red} are reflectance in the near-infrared and red wavebands, and has been shown to have a good correlation with vegetation productivity (Pettorelli *et al.*, 2005; Beck and Goetz, 2011). NDVI is also less prone to terrain illumination effects than other vegetation indices (Galvão *et al.*, 2016). NDVI values range from -1 to 1, where values near -1 indicate water bodies, values between 0 and 0.2 indicate bare surfaces, and values from 0.2 to 1 indicate increasing amounts of photosynthetically active plant biomass (Bonan, 2016).

Besides NDVI and its capacity to capture plant physiological activity, vegetation structure is also responsive to climate in a global scale. Vegetation stature and biomass allocation are directly correlated to changes in precipitation and soil water, with higher canopy height and higher values of biomass found in regions with greater values of annual rainfall. Because of

that, we incorporated in this study satellite-based canopy height and above ground biomass, hereafter AGB, measurements.

In this study we used AGB and canopy height satellite-based datasets that were produced using the same data source, which are the Geoscience Laser Altimeter System (GLAS) aboard the ICEsat spacecraft. Some of the objectives of the ICEsat mission are to measure cloud heights and the vertical structure of clouds and aerosols in the atmosphere, to map the topography of land surfaces, and to measure roughness, reflectivity, vegetation heights, snow-cover, and sea-ice surface characteristics. Despite having the same data source, AGB and canopy height used datasets, distinguish in their estimation's methods.

Canopy height estimations were based on the global dataset provided by Simard et. al (2011). This dataset was produced with GLAS data from May/2005 and June/2005, with the derived height metric RH100. The RH100 is a measure of the distance between the signal beginning and the ground peak for each GLAS waveform. GLAS waveforms are disturbed by sloped terrain, because of that, Simard et. al (2011) used Shuttle Radar Topography Mission (SRTM) data to remove from the analysis all waveforms that were located in areas of high slope (>5°) or where the slope correction was >25% of the measured RH100. After that, canopy height was estimated for each remaining waveform and extrapolated to produce a wall-to-wall map. This extrapolation was based on seven globally available variables: mean precipitation, precipitation seasonality, mean temperature, temperature seasonality, elevation, MODIS tree cover, and protection status.

AGB estimations were based on the pan-tropical biomass map provided by Avitabile et al (2016). This map was produced with a fusion of two other inputs biomass maps, from Saatchi et al (2011) and Baccini et al (2012). These two inputs maps are consistent in terms of

methodology because both use the same primary data source (GLAS LiDAR) alongside a similar modelling approach to upscale the LiDAR data to larger scales. Avitabile et al (2016) used a bias-removal approach by incorporating additional field observations and locally-calibrated high-resolution biomass maps. The inputs maps were fused by the method of weighted linear averaging. By this method, Avitabile et al (2016) was able to diminish the bias in the overall mean AGB, from 21 and 28 Mg ha^{-1} of the Saatchi et al (2011) and Baccini et al (2012) maps respectively, to 5 Mg ha^{-1} in the fused map.

2.4 Climatic water deficit and actual evapotranspiration as biologically meaningful variables

Vegetation distribution and water availability can be linked through hydroclimatic parameters meaningful to plant physiology, such as Actual Evapotranspiration (AET) and Climatic Water Deficit (CWD) (Stephenson, 1998). Both variables provide a reasonable biological interpretation, and have shown good correlation with the distribution of different vegetation types, from local to continental scales (Stephenson, 1998; Dilts *et al.*, 2015; Kane *et al.*, 2015; McIntyre *et al.*, 2015) (Figure 2a). Both CWD and AET estimate the length and magnitude of hydroclimatic conditions to plants; CWD is related to drought, and AET represents favorable conditions of biologically usable water availability and energy inputs to the environment (Stephenson, 1998). Therefore, assessing water availability by considering water and energy conservation variables (AET and CWD) could help overcome the issues imposed by data limitations on large scale studies of vegetation-hydrology coupling (Velpuri *et al.*, 2013; Baik and Choi, 2015).

We make use of the relationship between AET and CWD to provide a process-based analysis of the total amount of water and energy held in the system through time, according to the conceptual basis of the conservation of water (Equation 4) and energy (Equation 5):

(Eq. 4) $W = AET + S$

(Eq. 5) $PET = AET + CWD$

Where in Equation 4 *W* is available water and *S* is surplus, and in Equation 5 *PET* is potential evapotranspiration (Nathan L Stephenson, 1990).

AET estimates the simultaneous availability of water and energy usable by plants, which is related to the magnitude and length of favorable conditions to primary production. In contrast, CWD is related to the length and magnitude of stress experienced by plants, including heat stress that cannot be regulated by transpiration (Stephenson, 1998). This way, the relationship between AET and CWD allows us to not only estimate water availability in a system, but also assess the drivers of its variation, by plotting AET and CWD as perpendicular axes to infer the effects of changing evaporative demand and/or water availability in a given site (Stephenson, 1998) (Figure 3b).

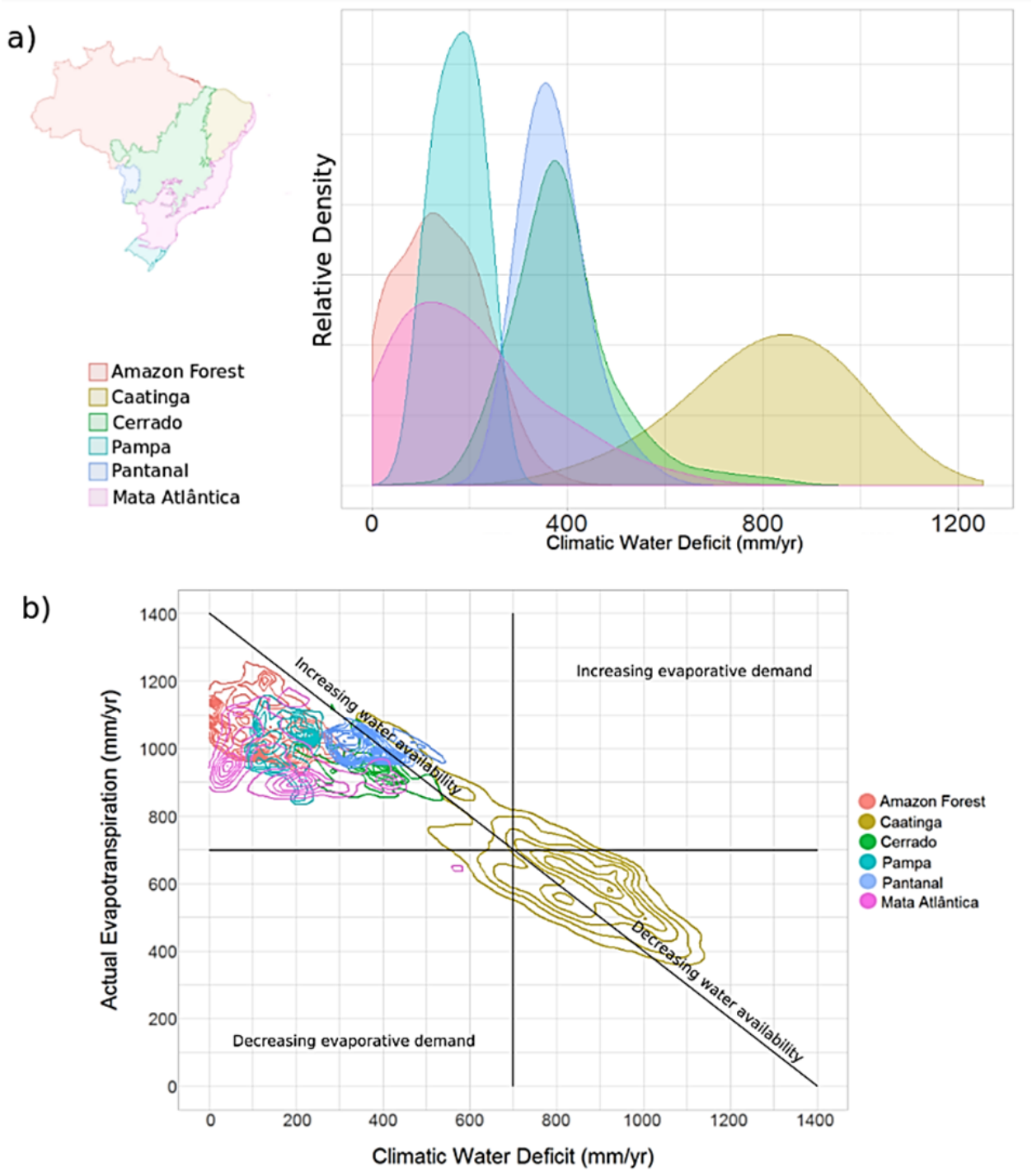

Figure 3: a) Density plot of the annual mean Climatic Water Deficit (CWD) of main Brazilian biomes; b) Actual Evapotranspiration (AET) and Climatic Water Deficit (CWD) mean annual (2000-2017) relationship density plot of Brazil's territory for each biome. Decreasing evaporative demand can decrease AET, CWD or both; the reverse holds for increasing evaporative demand. In contrast, changing water availability is limited to a diagonal line of slope -1 and *y*-intercept PET, because PET = AET + CWD; since a change in water availability does not affect PET alone, any increase in AET is mirrored by an equal decrease in CWD, and vice versa. CWD and AET annual data were acquired from the TerraClimate dataset, from 1958 to 2017.

3. METHODS

3.1 Study area

We studied the Espinhaço Mountain Range in eastern Brazil (Figure 4). The Espinhaço is the largest interior mountain range[1] in Brazil, and comprises one of the most ancient landscapes on Earth, having emerged during Gondwana formation and dating back to the Precambrian, nearly 640 Mya (Alkmin, 2012). This mountain range is the natural watershed divider between the *Atlântico Leste* (AL), *São Francisco* (SF) and *Atlântico Sudeste* river basins.

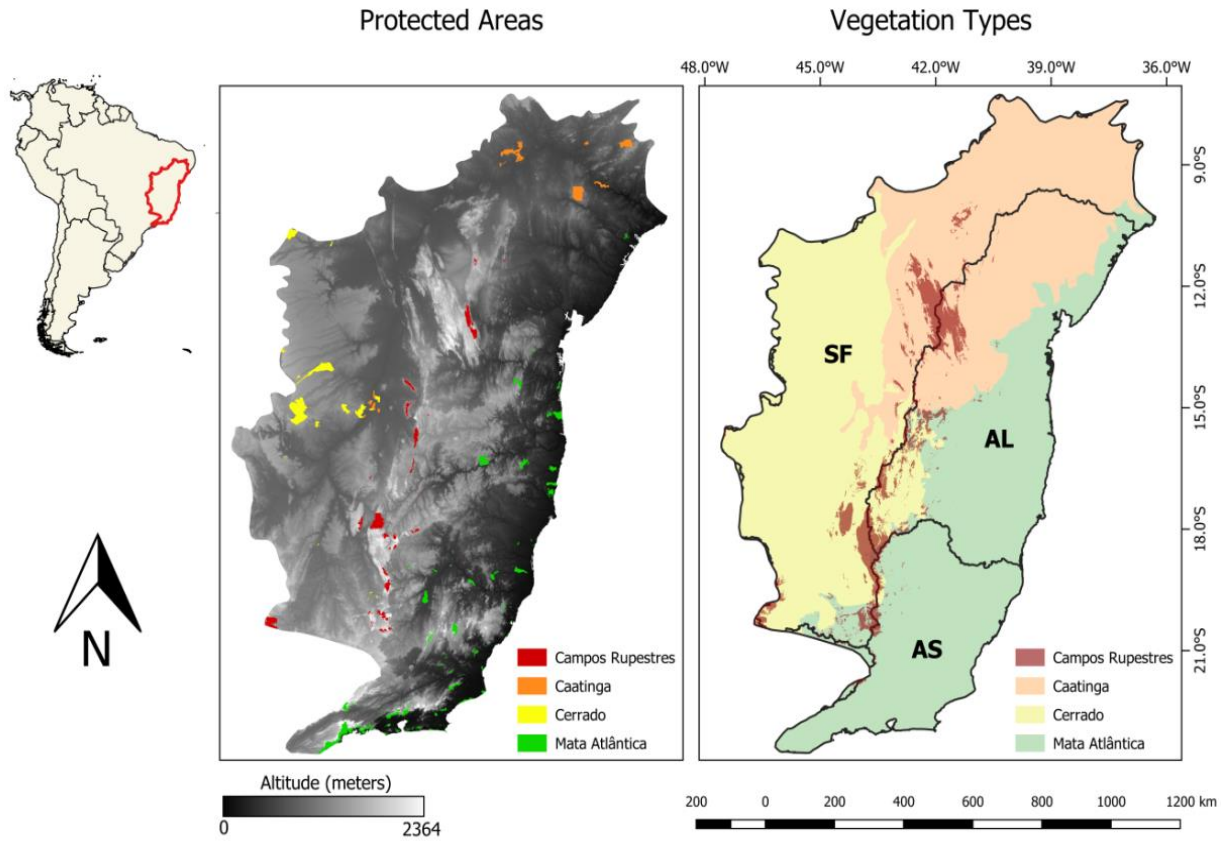

Figure 4: Overview of the Espinhaço mountain range in Brazil. On the left panel, the topography and extent of the Espinhaço Mountain Range and the protected areas classified by vegetation types, in Brazil.

[1] Mountains are often defined by a geological connotation, being structures that has been disturbed through folding, uplift or volcanism (Meybeck, Green and Vörösmarty, 2001; Viviroli *et al.*, 2007). In this study, we use an ecological definition of mountains, being structures with high topographic variation where ecosystems are controlled by the relationship of elevation, topography and hydroclimate (Körner *et al.*, 2017).

On the right, the Espinhaço Range as an ecotone of vegetation types (MMA, 2015), and as the watershed of São Francisco (SF), Atlântico Leste (AL) and Atlântico Sudeste (AS) basins.

At finer scales, the roughness of the Espinhaço topography and its acute features creates a variety of soil types and depths, microclimates and special environmental conditions, which harbor a mosaic of vegetation types with remarkably high species diversity and endemism rates (Silveira *et al.*, 2016). This diversity is also a result of its historical climatic stability, which may have favored species establishment by promoting refugia under unfavorable climates, following the old climatically-buffered infertile landscapes" (OCBILs) theory (Benites *et al.*, 2007; Hopper, 2009; Silveira *et al.*, 2016).

At the continental scale, the location of the Espinhaço range places it at the ecotone of three major biomes: Atlantic Forest to the east and Cerrado savannas to the west, both global biodiversity hotspots (Myers *et al.*, 2000), and Caatinga dry forests to the north. The Atlantic Forest at eastern Espinhaço slopes is composed by tropical forest vegetation, with coastal humid evergreen rainforests transitioning towards interior semi-deciduous forests (Morellato *et al.*, 2000). The western Espinhaço is covered by Cerrado, the most species-rich tropical savanna in the world, with vegetation types ranging from grasslands to woodlands (Simon *et al.*, 2009). At the northern portions, between the limits of AL and SF basins, the vegetation is an ecotone of Cerrado and dry woodlands, transitioning into the Caatinga biome, unique to NE Brazil (Portillo-Quintero and Sánchez-Azofeifa, 2010). The Espinhaço highlands are dominated by *Campos Rupestres* (rupestrian grasslands), a montane vegetation mosaic dominated by fire-prone grasslands growing at high elevations (> 900 meters a.s.l.) on shallow stony and/or waterlogged sandy soils, with scattered quartzite or ironstone rocky outcrops dominated by shrubs, and gallery forests and relictual hilltop forest patches (Silveira *et al.*, 2016).

Precipitation has a latitudinal pattern along the Espinhaço Range, with decreasing total annual rainfall towards the north. Annual precipitation ranges from 480 mm/year to 1520 mm/year (Figure 5a), and is highly seasonal, with the dry period corresponding to the Autumn-Winter months (April to September). There is no significant difference in the amount of rainfall between AL and SF (east to west), despite the potential orographic effects at the highest elevations (Fernandes, 2016). Remarkably, although no differences in rainfall volume between east and west Espinhaço are found, annual cloud cover frequency is significantly higher at the eastern side and over mountaintops of the meridional Espinhaço, impacting light availability (Streher et al. 2017). Daytime mean temperatures show both latitudinal and longitudinal patterns. The latitudinal pattern is opposite to rainfall, with higher temperatures in the northern region, c.a. 5°C warmer than the southern portion. The longitudinal pattern shows higher temperatures on the western side (30.6 ± 2.2 °C) compared to the east (26.6 ± 2 °C) (Figure 5b).

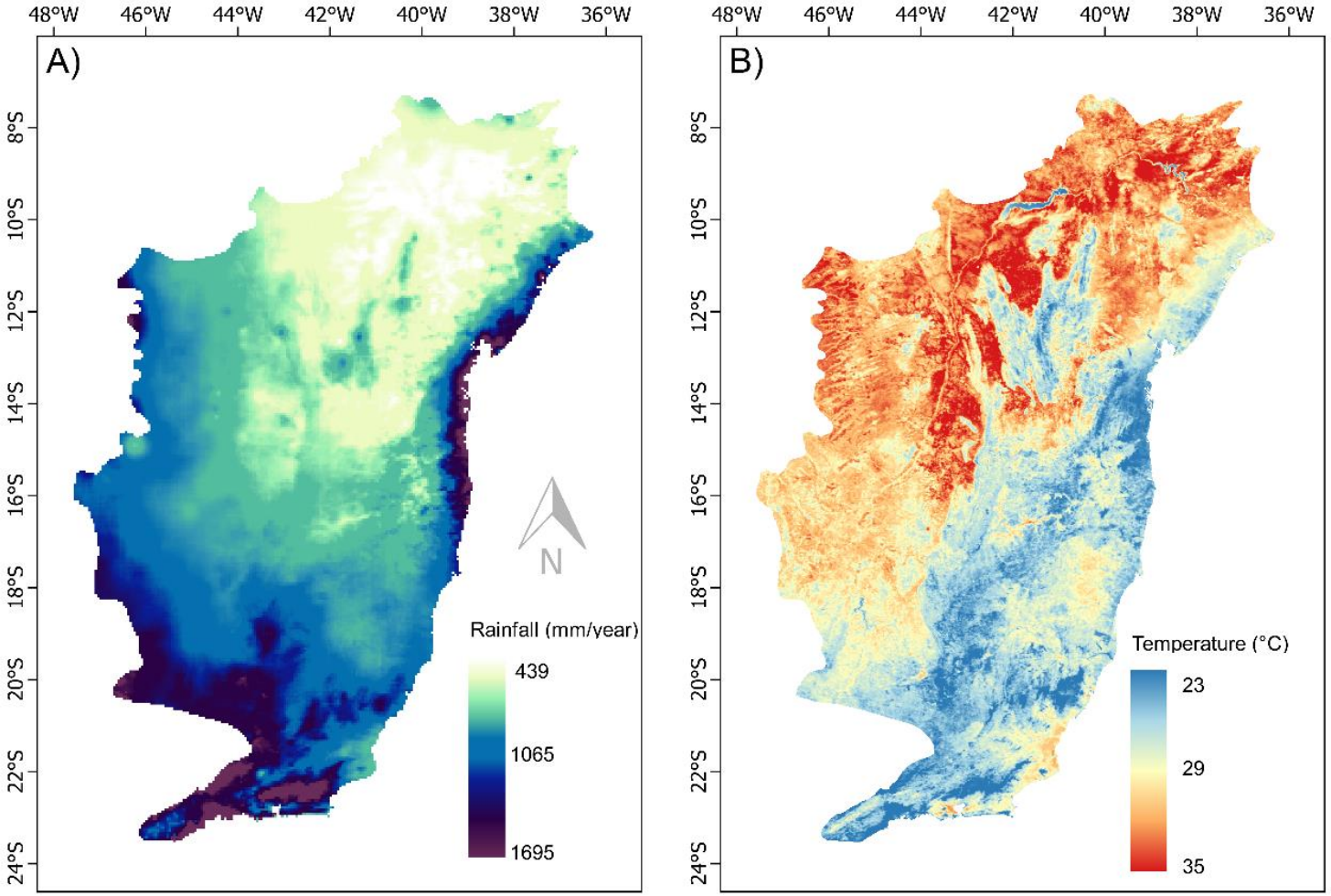

Figure 5: A) Mean annual rainfall from the CHIRPS 1981-2017 precipitation dataset time series for the Espinhaço Range. B) Mean daily surface temperature from the MODIS/LST 2000-2017 product for the Espinhaço Range (Sobreiro, Streher and Silva, 2017).

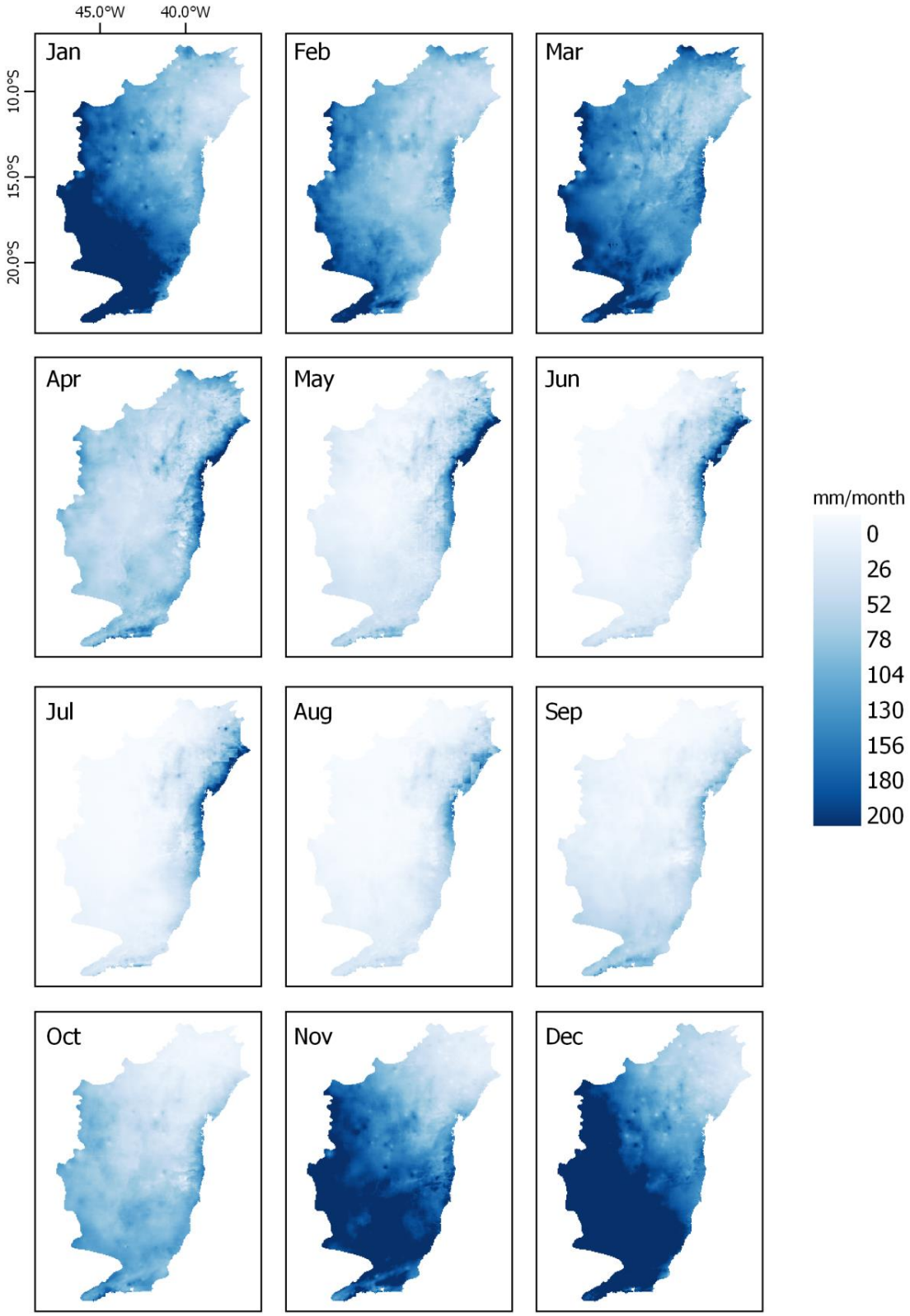

Figure 6: Mean monthly rainfall from the CHIRPS 1981-2017 precipitation dataset time series for the Espinhaço Range (SOBREIRO, 2015).

3.2 Remotely sensed hydroclimatic dataset

We used the TerraClimate dataset (Abatzoglou *et al.*, 2018) as a measure of AET and CWD values, which are gridded (~ 4km) monthly data products of AET and CWD from 1958 to 2017. TerraClimate products are generated from the interpolation of different global weather station databases from WorldClim (version 1.4 and version 2.0), CRU Ts4.0 and JRA-55. Potential Evapotranspiration (PET) is calculated using the Penman-Montieth approach (Allen *et al.*, 1998). To calculate AET and CWD, TerraClimate uses a one-dimensional modified Thornthwaite-Mather (1955) climatic water-balance model (Lutz, van Wagtendonk and Franklin, 2010) which incorporates soil water-holding capacity, slope and aspect, with CWD given as the difference between Potential Evapotranspiration (PET) and Actual Evapotranspiration (AET).

3.3 Remotely sensed vegetation datasets

3.3.1 Moderate resolution imaging spectroradiometer (MODIS) - NDVI

We used a time-series of 204 NDVI images generated from the Moderate Resolution Imaging Spectroradiometer (MODIS). We used MODIS product NDVI/MOD13A3 Version 6 with 1km resolution (Didan, 2015), covering the interval between January/2001 and December/2017, at monthly intervals. Data was obtained from the Land Process Distributed Active Archive Center (LP-DAAC – USGS/NASA). Monthly NDVI pixels values result from the best pixel composite of two 16-day composite periods. In order to improve the quality of pixels, and minimize atmospheric and cloud effects, the 16-day period algorithm chooses the best available pixel within all the acquisition dates. All monthly images were downloaded, mosaiced and transformed to GeoTIFF format using the "MODIStsp" package of the R programming language (R Core Team, 2013; Busetto and Ranghetti, 2016).

3.3.2 Aboveground Biomass and Forest Canopy Height datasets

To assess the spatial relationship between vegetation distribution and CWD and AET we used the datasets of Aboveground Biomass (AGB) and Forest Canopy Height, from Avitabile et al (2016) and Simard et al (2011) respectively, as variance in these traits is expected to be responsive to climate patterns. We obtained AGB values from the Pan-tropical biomass map by Avitabile et. al (Avitabile *et al.*, 2016) with 1-km spatial resolution. The AGB map is freely available at the Wageningen University & Research website (https://www.wur.nl). The canopy height dataset is also freely available from the Spatial Data Access Tool (SDAT) at the Oak Ridge National Laboratory Distributed Active Archive Center (ORNL DAAC) website (webmap.ornl.gov/ogc/datasets).

Both AGB and canopy height datasets were also used to assess possible anomalies on their distribution and the AET and CWD mean annual values. Anomalies were characterized by a graphical analysis of the distribution of these variables within the AET and CWD bidimensional space, identifying regions that contradicted the expected pattern of higher AGB and Canopy Height in areas with high AET and low CWD, or vice-versa.

3.4 Topo-edaphic remotely sensed datasets

Elevation was derived from the Shuttle Radar Topography Mission (SRTM) 3-arcsec (90 m) dataset (± 15 m vertical accuracy), obtained from the Earth Explorer server of the United States Geological Survey (http://earthexplorer.usgs.gov/). To assess the topo-edaphic constraints on water availability we used the topographical wetness index (TWI), which is a relative measure of the potential long-term soil water storage capacity at a given site in the landscape (Title and Bemmels, 2018).

The TWI calculation is based on elevation, topographic slope and specific catchment area, which describes the tendency of the site to both receive water from upslope areas and retain this

water as a function of local slope. We used the TWI provided by the Environmental Rasters for Ecological Modeling (ENVIREM) project, which is calculated as a tangent function of slope angle, β, and specific catchment area, SCA (Equation 6) (Bohner and Selige, 2002). The catchment area is the discharge contributing upslope area of each grid cell (m^2) and the SCA is the corresponding drainage area per unit contour width ($m^2.m^{-1}$).

$$\textbf{(Eq. 6)} \quad TWI = \ln\left(\frac{SCA}{\tan\beta}\right)$$

TWI was downloaded from the Environmental Rasters for Ecological Modeling (ENVIREM) project (Title and Bemmels, 2018) which is freely available at http://envirem.github.io. All products were resampled to 1km spatial resolution to match vegetation and hydroclimatic datasets using the "raster" package (Hijmans, 2017) implemented in R (R Core Team, 2013).

3.5 Actual evapotranspiration and climatic water deficit classification into hydroclimatic classes

To define the hydroclimatic regions of the study region and assess the spatial patterns of relationship between AET and CWD and the vegetation we performed an unsupervised *k-means* classification. All the following analysis were then based on the generated hydroclimatic classes as they represent the spatial dimension of the relationship between vegetation and hydroclimate.

We used as inputs to the *k-means* classification the average annual mean CWD, average annual standard deviation of CWD, the average annual 90^{th} percentile of AET and average 10^{th} percentile of AET, as well as they average annual standard deviations, for a total of 6 layers. AET percentiles were calculated for each year of the time-series (2001 – 2017), and then summarized into their mean time-series values and standard deviations. These variables were chosen to capture both the intra-annual seasonality and interannual variability of AET and

CWD over the time-series (2001 to 2017), and to eliminate possible measurement errors such as extreme values.

The *k-means* classification algorithm is commonly used to partition data automatically. The procedure begins with the selection of *k* grouping centers and then iteratively refining them by minimizing within-class distances and maximizing between-class distances. The algorithm converges when there are no more changes between the instances for grouping centers (Wagstaff *et al.*, 2001), following a predefined threshold. The unsupervised *k-means* classification was performed in the R software using the *kmeans* function within the R Stats Package (R Core Team 2013).

3.6 Seasonal (intra-annual) response of NDVI to CWD variations

We implemented a pixel-wise 4-parameter sinusoidal model for the NDVI and CWD time series (Equation 7), following Jones et al. (2014). This method provides a phase shift parameter (c) that quantifies the temporal offset between the two series (Jones, Kimball and Nemani, 2014). The temporal offset in months was calculated as the phase shift difference divided by 2π/b; b in all cases was equivalent to 12, confirming a yearly cycle, as datasets had a monthly temporal resolution.

$$\textbf{(Eq. 7)} \quad y_{t=y_0+a\left(\frac{2\pi x}{b}+c\right)}$$

Where yt is the fitted monthly climatology value, y0 is the mean value, a is the amplitude of the sinusoidal curve, x is the monthly increment, b is the frequency, and c is the phase shift.

To assess the degree of coupling between CWD and NDVI, and therefore NDVI responses to water availability, we subtracted the phase shift (c) difference of CWD and NDVI time-series model results. The values of phase shift differences can be interpreted as the time, in months,

in which the maximum value of NDVI lagged the time of minimum evaporative demand not met by vegetation transpiration, here expressed by the lowest value of CWD.

3.7 Interannual responses of NDVI to annual CWD anomalies

To assess the vegetation sensitivity to year-to-year fluctuations of water availability, we performed an analysis based on the relationship of annual CWD anomalies and the vegetation class phase shift differences. CWD anomalies were calculated as the difference between the climatological mean annual CWD (1958 -2017) and annual CWD (2001 - 2017) (Equation 9), in this way negative values represents a drier year and positive values a wetter year, when compared to the CWD climatological mean.

$$\textbf{(Eq. 9)}\ CWD_{anomaly} = CWD_{mean(1958-2017)} - CWD_{year}$$

where *year* is the annual CWD from 2001 to 2017.

We fitted the Equation 7 model separately for each year, from 2001 to 2017, for the NDVI and CWD time series. This allowed us to have a coupling value (phase shift difference) for each year of the analyzed series. After that, we fitted linear regressions between the set of annual CWD anomalies and its correspondent phase shift difference values, for immediate responses and for a 1-year lag response, since vegetation response to CWD may be observed with a delay. The linear regressions were also fitted separately for different intervals of TWI, to capture possible topo-edaphic influences on vegetation sensitivity to CWD fluctuations. We expected that the higher the determination coefficient (r^2), the more the vegetation water use strategy was sensitive to CWD anomalies.

3.8 Natural vegetation mask

Land cover on the study area has been historically and heavily disturbed by human activities, such as urbanization, deforestation, agricultural appropriation (i.e. Eucalyptus and Pinus

plantations, soybean and sugar cane crops), wood extraction and opencast mining (Silveira *et al.*, 2016). To ensure we were assessing the responses of natural vegetation in relation to water availability, we assembled a 2017 land use and land cover map from the MapBiomas Version 3.0 initiative, which is a multi-institutional model to generate annual land cover and uses maps from an automatic classification processes applied to satellite images (Projeto MapBiomas, 2019). The complete description of the product and methods can be found at http://mapbiomas.org.

We reclassified the MapBiomas 2017 land use and land cover map to native vegetation areas and anthropic areas, and then resampled it to 1km x 1km resolution recording the proportion of native vegetation within each 1km cell, from the original 30m resolution. We then eliminated the pixels with less than 70% of native cover, and used the remaining pixels as our natural vegetation areas mask (Figure 7).

Vegetation types were classified following the Brazilian official biome classification, and then attributed to the raster of natural areas. To delineate the "Campos Rupestres" classification, which is not an official biome, we identified all native vegetation areas that overlaid the Silveira et. al (2016) "Campos Rupestres" delineation, and reclassified it as "Campos Rupestres" natural areas. The vegetation types found on the study area are, hereafter, classified as "Caatinga" (257.096 pixels), "Campos Rupestres" (59.755 pixels), "Cerrado" (290.047 pixels) and "Mata Atlântica" (131.138 pixels).

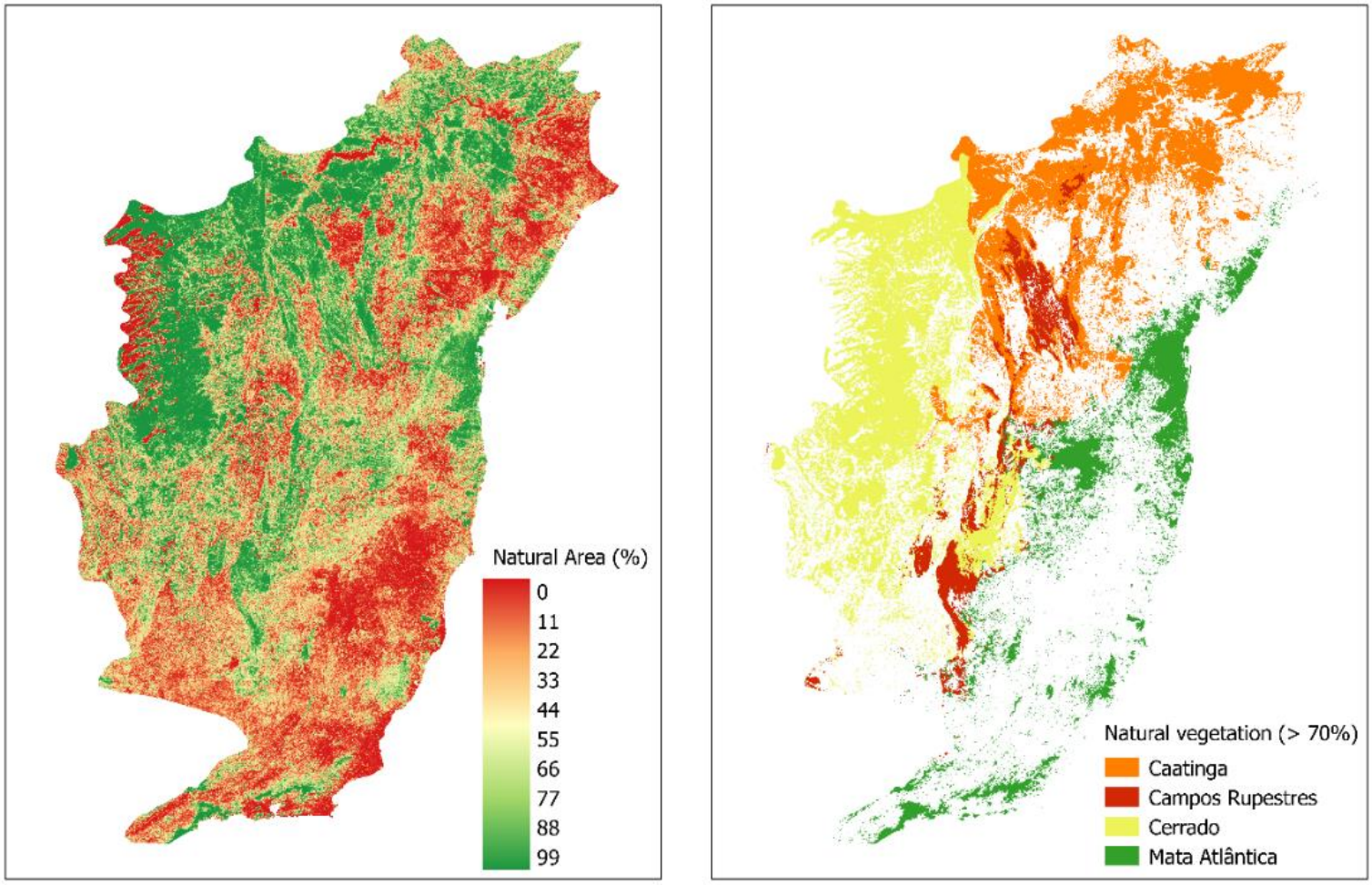

Figure 7: In the left panel, resampled to 1km MapBiomas land use (2017) dataset; each pixel corresponds to a percentage of natural vegetation within the resampled spatial resolution. In the right panel, the mask of > 70% natural vegetation within a resampled pixel, and classified as the biomes in the study area.

4. RESULTS

4.1 Which are the hydroclimatic regimes found and their correspondent vegetation types?

The unsupervised *k-means* classification of AET and CWD seasonal mean patterns resulted in an ideal number of 6 classes. After testing the algorithm for different number of classes, based on our previous knowledge of the studied region, the 6 classes definition presented as the best hydroclimatic representation since did not over fragmented the regimes or underestimated the hydroclimatic relations. The 6 resulting classes were named after their main hydroclimatic characteristic, given by the seasonal mean patterns of AET and CWD, as follow: "*Humid*", "*Semi humid*", "*Wet seasonal*"," "*Dry seasonal*", "*Dry*" and "*Very dry*" (Figure 8b). We found both longitudinal and latitudinal moisture patterns. The northern and western regions were drier, consistent with precipitation regimes and sea influence in the east coast.

"*Humid*" and "*Very dry*" classes had the smallest seasonality of AET and CWD, the first with high AET (76 ± 22 mm/month) and low CWD (12 ± 11 mm/month) throughout the year, while the opposite pattern was observed for the "*Very dry*" class, with low AET (35 ± 27 mm/month) and high CWD (97 ± 30 mm/month) (Figures 8 and 9). The "*Semi humid*" class showed similar AET (70 ± 26 mm/month) values to the "*Humid*" class, but differed in having higher values of CWD (26 ± 17 mm/month). This same pattern held for the differentiation between "*Wet seasonal*" and "*Dry seasonal*" classes, both with large AET ("*Wet seasonal*" = 72 ± 35 mm/month; "*Dry seasonal*" = 63 ± 38 mm/month) and CWD ("*Wet seasonal*" = 42 ± 37 mm/month; "*Dry seasonal*" = 58 ± 37 mm/month) seasonality over the year, with "*Dry seasonal*" showing the highest CWD values. Despite the low annual AET (37 ± 17 mm/month), the "*Dry*" class had small variation in AET values across the year, which was the main factor

for its differentiation from the "*Very dry*" class, which experienced near 0/mm in several months (Figure 8 and 9).

Within the classical biome distribution, we found that topography was an important factor by delimiting different hydroclimatic regimes in a drier region (Figure 9). In the northern Espinhaço, we found a "*Wet seasonal*" area within the "*Dry*" seasonal class, which is clearly related to the higher elevations found on that region, known as *Chapada Diamantina*, where elevation is c.a. 1400 meters a.s.l. (Figure 4). However, elevation was not a factor for hydroclimatic delimitation in the southern Espinhaço, since eastern meridional portions of "*Cerrado*" in the Espinhaço lowlands experienced the same "*Semi humid*" hydroclimatic regime, which is mostly characterized by "*Mata Atlântica*" presence (Figure 9).

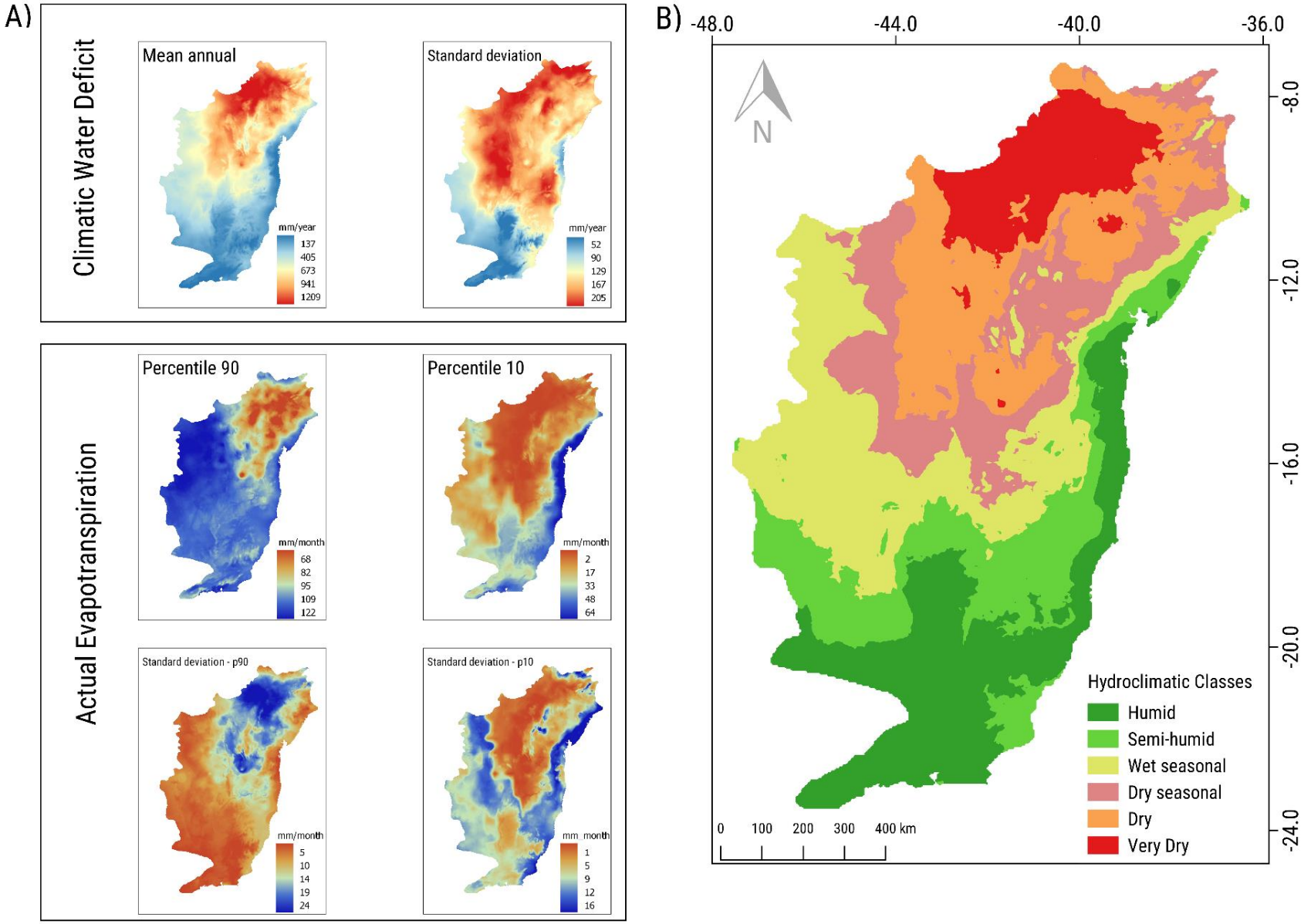

Figure 8: A) Spatial mean patterns of AET (90 and 10 percentile) and CWD (annual mean) and their standard deviation. The six layers were used for the unsupervised k-means classification. B) Hydroclimatic classes generated from the unsupervised k-means classification.

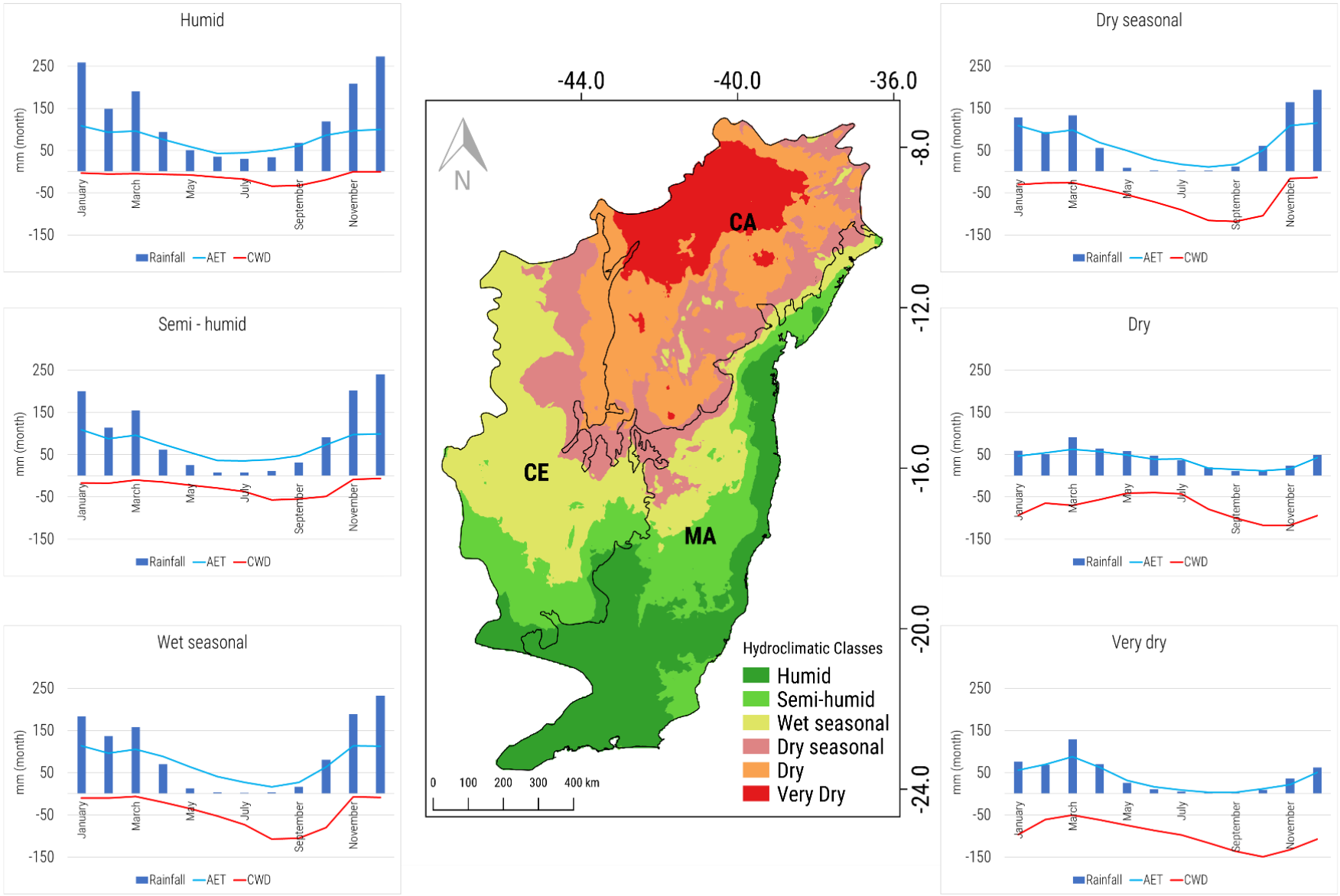

Figure 9: Hydroclimatic classes generated from the unsupervised k-means classification and classical biome delimitation, where the black lines represent the classic Brazilian biome distribution and "CE" is *Cerrado*, "MA" is *Mata Atlântica* and "CA" is *Caatinga*. Left and right panels show climographs for each Hydroclimatic class, with their respective means (2001-2017) for AET, CWD (multiplied by -1) and rainfall.

4.2 Where does vegetation productivity is more and/or less coupled to hydroclimatic regimes?

The sinusoidal model of NDVI and CWD coupled climatology had different phase shifts for "*Caatinga*" and "*Mata Atlântica*", whilst "*Cerrado*" and "*Campos Rupestres*" shared similar phase shift patterns (Table 1; Figure 10).

Table 1: Mean phase shift difference (in months) values and their standard deviation inside brackets for each vegetation analyzed and their respective distribution into the Hydroclimatic classes. The "X" represents that there were no observations for a given vegetation class and the correspondent Hydroclimatic class.

	Humid	**Semi-humid**	**Wet seasonal**	**Dry seasonal**	**Dry**	**Very Dry**
Caatinga	X	X	X	0.3 (±0.7)	0.2 (±0.4)	0.0 (±0.3)
Campos Rupestres	1.6 (±0.5)	1.4 (±0.4)	1.3 (±0.6)	0.9 (±0.7)	0.7 (±0.3)	0.3 (±0.3)
Cerrado	1.4 (±0.4)	1.3 (±0.4)	1 (±0.4)	0.7 (±0.3)	0.4 (±0.3)	0.5 (±0.5)
Mata Atlântica	0.6 (±1.6)	0.2 (±1.6)	1.1 (±1)	X	X	X

The phase shift difference between CWD and NDVI varied regarding the vegetation type and hydroclimatic region, with a general pattern of increased phase shift difference from drier to

moist regions. Positive values are equivalent to how long, in months, the maximum NDVI was expressed after the minimum CWD, and negative values are equivalent of how long, in months, maximum NDVI preceded minimum CWD (Table 1; Figure 10).

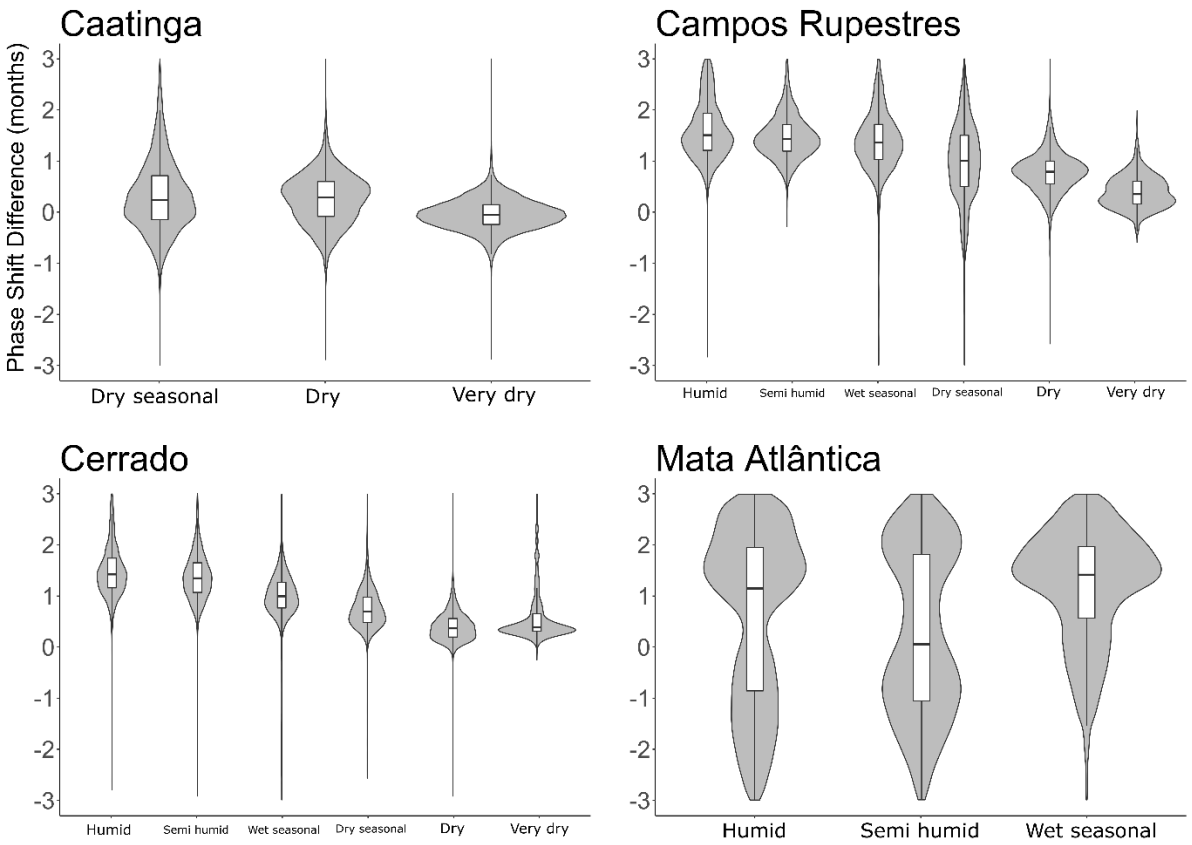

Figure 10: Phase shift difference (in months) for the vegetation types and their respective Hydroclimatic classes as boxplots, indicating the median and quartiles. The violin plot outlines illustrate kernel probability density, i.e. the width of the shaded area represents the proportion of the data located there.

"*Caatinga*" had a mean pattern of NDVI peaks responding almost immediately to CWD in all hydroclimatic classes, ranging from 0.3 months to immediate response, 0 months. (Table 1; Figure 10). "*Campos Rupestres*" and "*Cerrado*" showed a gradient of coupling, from higher phase shift difference values in moister regions, 1.6 months and 1.4 months respectively, to lower values in drier regions, 0.3 months and 0.5 months respectively (Table 1; Figure 10). "*Mata Atlântica*" phase shift difference values were highly variable in all Hydroclimatic classes analyzed, with standard deviation reaching 8 times the mean value in the "*Semi humid*" class (Table 1; Figure 10).

4.3 Is topography able to impact vegetation productivity and its coupling relations to hydroclimatic regimes?

The "*Caatinga*" vegetation distribution spanned the "*Very dry*", "*Dry*" and "*Dry seasonal*" classes, marked by low water availability and high-water deficit, with strong seasonality within the "*Dry seasonal*" region. We found low AGB (13.8 ± 25.7 Pg/km²) and higher canopy height (4.4 ± 4.9 m) in moister regions with higher AET and lower CWD (Figure 11). Most of "*Caatinga's*" natural vegetation sites are located in the São Francisco river lowlands with high TWI values (11.3 ± 1.3, unitless) and low elevations (603 ± 232 m).

"*Campos Rupestres*", which follow the S-N direction of the Espinhaço Range, covered all hydroclimatic classes. With low AGB (24.4 ± 36.9 Pg/km²) and low canopy height (4.8 ± 6.4 m), as well as low TWI (9.6 ± 0.8, unitless), a result of the larger topographic variance on mountaintops (1077 ± 152 m), "*Campos Rupestres*" experiences relatively high AET, low CWD and strong seasonality when compared to other vegetation classes, with the exception of small areas located in the "*Dry*" and "*Very dry*" classes (Figure 11).

"*Cerrado*" had small values of AGB (19.1 ± 28.7 Pg/km²), larger values of canopy height (5.9 ± 5.1 m) and relative topographic uniformity, with high TWI values (11.5 ± 1.2, unitless) occupying medium elevation regions (711 ± 177 m), with most of its sites experiencing high water availability with strong seasonal fluctuations within the "*Wet seasonal*" class, despite occupying all hydroclimatic regions (Figure 11).

"*Mata Atlântica*" occupied the widest range of environmental conditions regarding all vegetation and topographic variables analyzed (TWI = 10.1 ± 1.3 unitless; elevation = 555 ± 390 m), mostly because its distributional range accounts for two major diverging regions, the coast and the Espinhaço's eastern lowlands. As it is widely known and expected, "*Mata Atlântica*" had the highest values of AGB (114.9 ± 67.4 Pg/km²) and canopy height (15.6 ± 8.4 m) within all vegetation types (Figure 11).

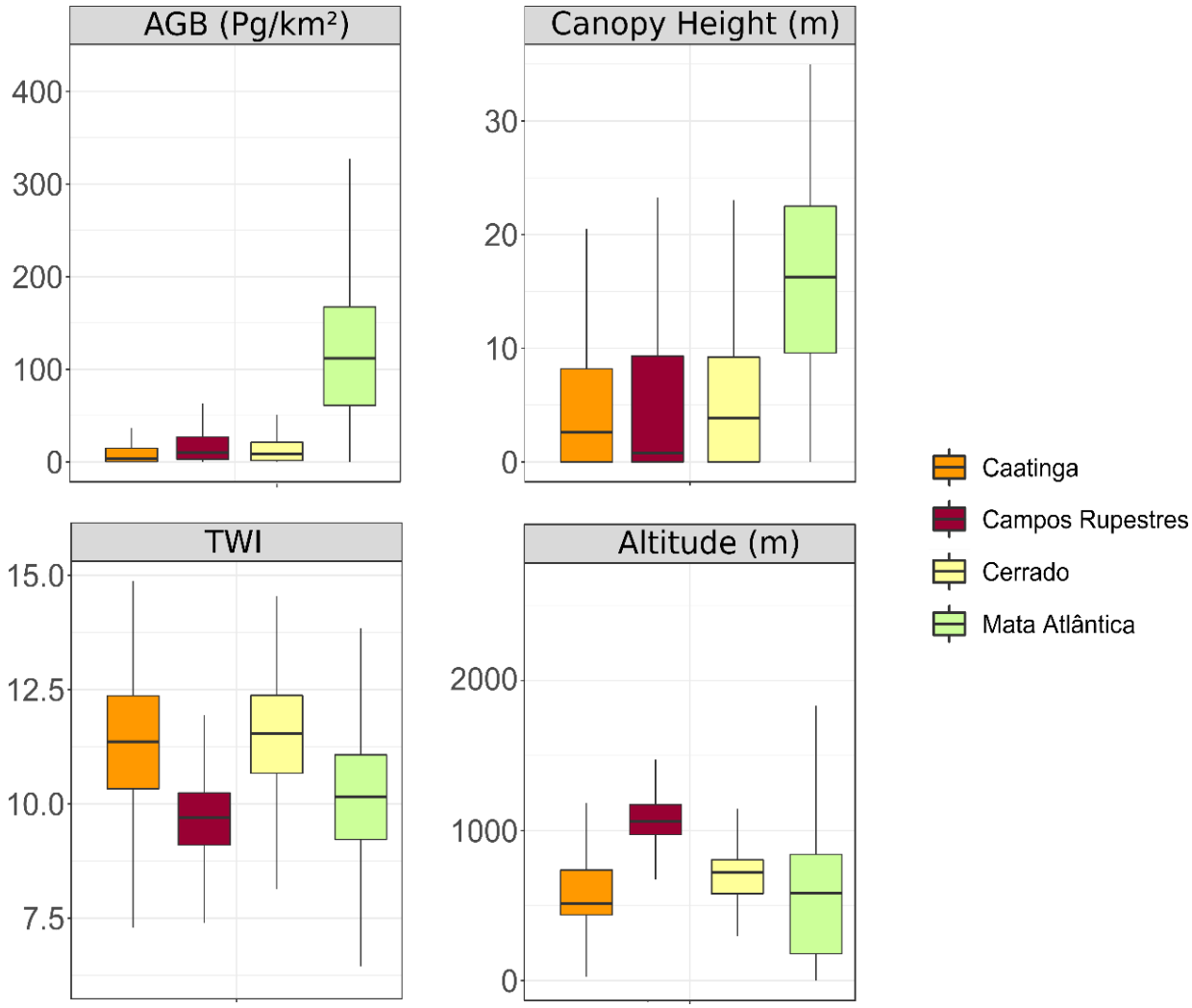

Figure 11: Boxplot of the vegetation structure (Aboveground Biomass and Canopy Height) and topographic (Topographic Wetness Index – TWI and Elevation) values found for each vegetation type analyzed.

We found anomalies regarding "*Cerrado*" (A1 and A2) and "*Mata Atlântica*" (A3 and A4) AGB and canopy height distribution and CWD-AET relations (Figures 12 and 13; Table 2). A1, where a low AGB-canopy height region was related to high AET and low CWD, is located in the southern Espinhaço highlands, at the "*Wet seasonal*" and "*Semi humid*" transition, where there is high water availability and rugged topography. A2, where higher AGB and canopy height vegetation was located in a region with lower water availability and higher deficit, was found on the "*Wet seasonal*"/"*Dry seasonal*" transition, an area characterized by the presence of the smooth lowlands of the São Francisco River. A3 was found in a region with high water

availability within the "*Humid*" and "*Semi humid*" classes, but with shorter trees and low values of AGB. A4 showed an abnormally low AGB and canopy height value within a region with high AET and medium to low CWD.

Table 2: Anomalies of hydroclimatic and vegetation structure association

ANOMALY	AET (MM/YEAR)	CWD (MM/YEAR)	AGB (PG/KM²)	CANOPY HEIGHT (METERS)
A1	915 ± 5	184 ± 4	5.5 ± 11.6	0.2 ± 1.3
A2	724 ± 37	756 ± 61	75.4 ± 47.4	12.6 ± 3.3
A3	825 ± 67	413 ± 88	56.9 ± 63.4	7.4 ± 7.8
A4	543 ± 21	616 ± 36	28.1 ± 26.4	10.3 ± 6.8

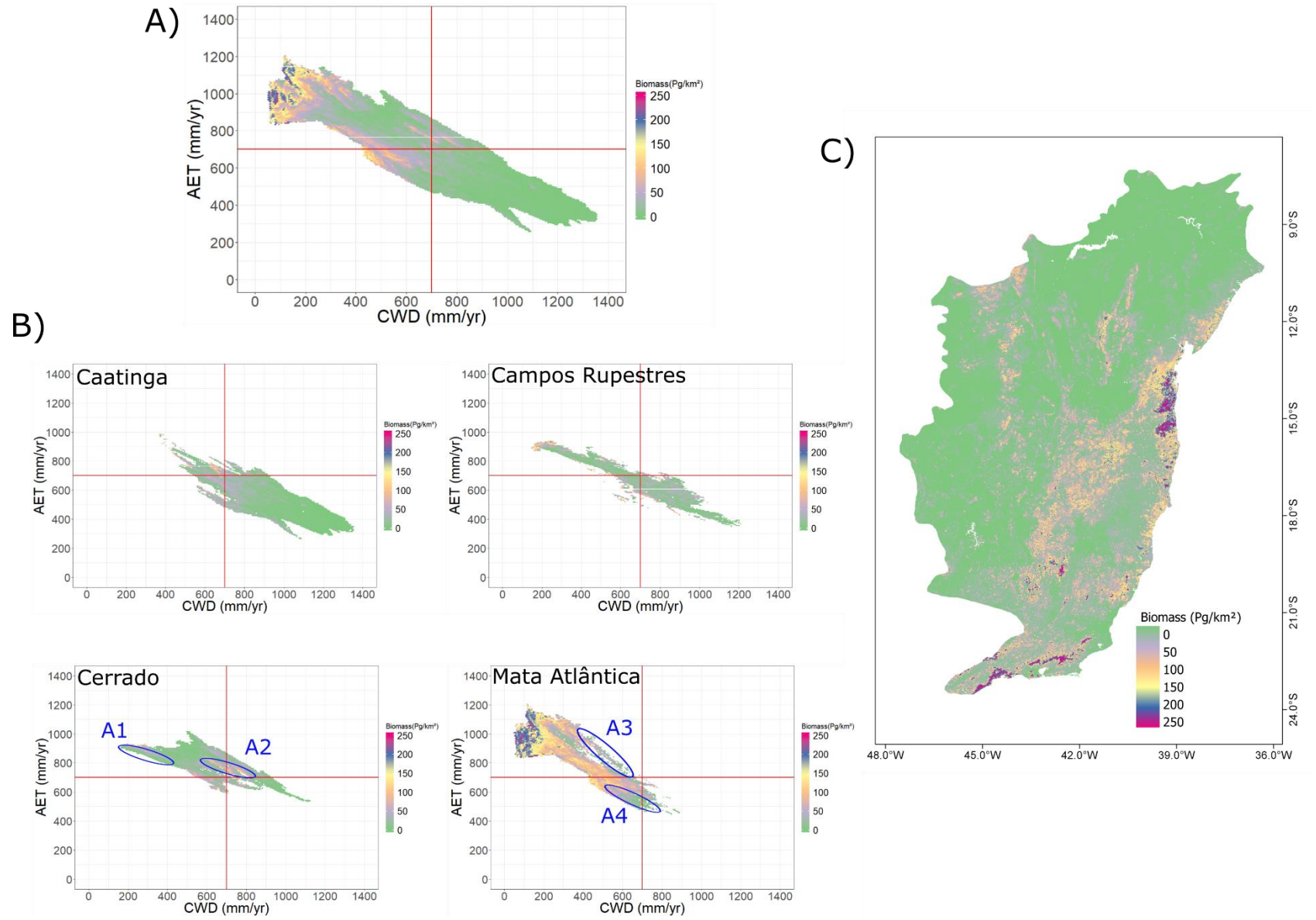

Figure 12: A) Actual evapotranspiration (AET) and Climatic Water Deficit (CWD) hexbin plots for the entire study area, and their relation with Aboveground Biomass (AGB - Pg/km²). Each bin corresponds to the mean of AGB for a user-defined certain amount of raster pixels. B) The same relation showed in A but for each vegetation type analyzed. Blue circles indicate the anomalies found on those relations (described in the text). C) Spatial distribution of AGB across the study area.

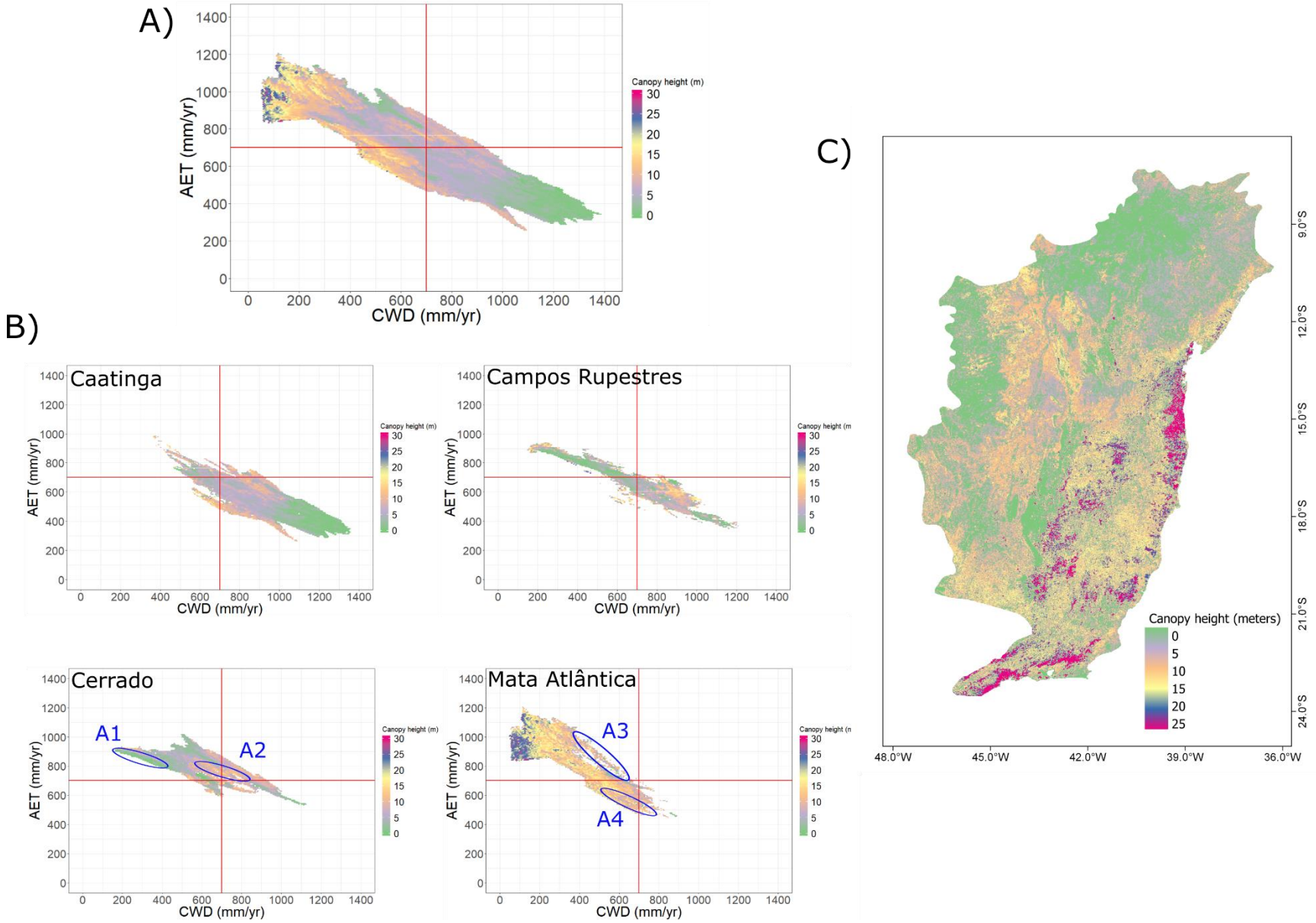

Figure 13: A) Actual evapotranspiration (AET) and Climatic Water Deficit (CWD) hexbin plot for the entire study area, and their relation with Canopy Height (meters). Each bin corresponds to the mean of AGB for a user-defined certain amount of raster pixels. B) The same relation showed in A but for each vegetation type analyzed. Blue circles indicate the anomalies found on those relations (described in the text). C) Spatial distribution of Canopy height across the study area.

4.4 What is the climatic resilience of the vegetation formations in this region?

We found the same patterns of positive (wetter years) and negative (drier years) anomalies across the hydroclimatic classes, being that the amplitude of the anomalies is greater within drier regions, showing a pattern of more extreme interannual climatic variability in the northern portion of the study area (Figure 14).

"*Caatinga*" CWD and NDVI coupling did not seem, over the analyzed years, to be influenced by CWD anomalies. For "*Campos Rupestres*", which encompassed all hydroclimatic classes, coupling seasonality was more responsive to annual anomalies in the "*Dry seasonal*" (TWI 10.1 to 12: $r^2 = 0.22$) and "*Dry*" with a 1-year lag (TWI 12.1 to 14: $r^2 = 0.29$) classes when experiencing topo-edaphic conditions favorable to water accumulation (Figure 15). When experiencing "*Humid*" (TWI 8.1 to 10: $r^2 = 0.17$) and "*Semi humid*" (TWI 6 to 8: $r^2 = 0.28$) classes and lower values of TWI, "*Cerrado*" was more sensitive to annual anomalies with a higher correlation for a 1-year lag (Figure 15).

"*Mata Atlântica*" showed the highest correlations among all biomes analyzed between the phase shift difference and CWD annual anomalies (Figure 15). Within the "*Humid*" (TWI 12.1 to 14: $r^2 = 0.36$) and "*Semi humid*" (TWI 12.1 to 14: $r^2 = 0.34$) classes, the highest correlations were found for a 1-year lag response and high TWI values, while for "*Wet seasonal*" class the highest coefficient was found for an immediate response at sites with TWI values ranging from 10.1 to 12 ($r^2 = 0.25$).

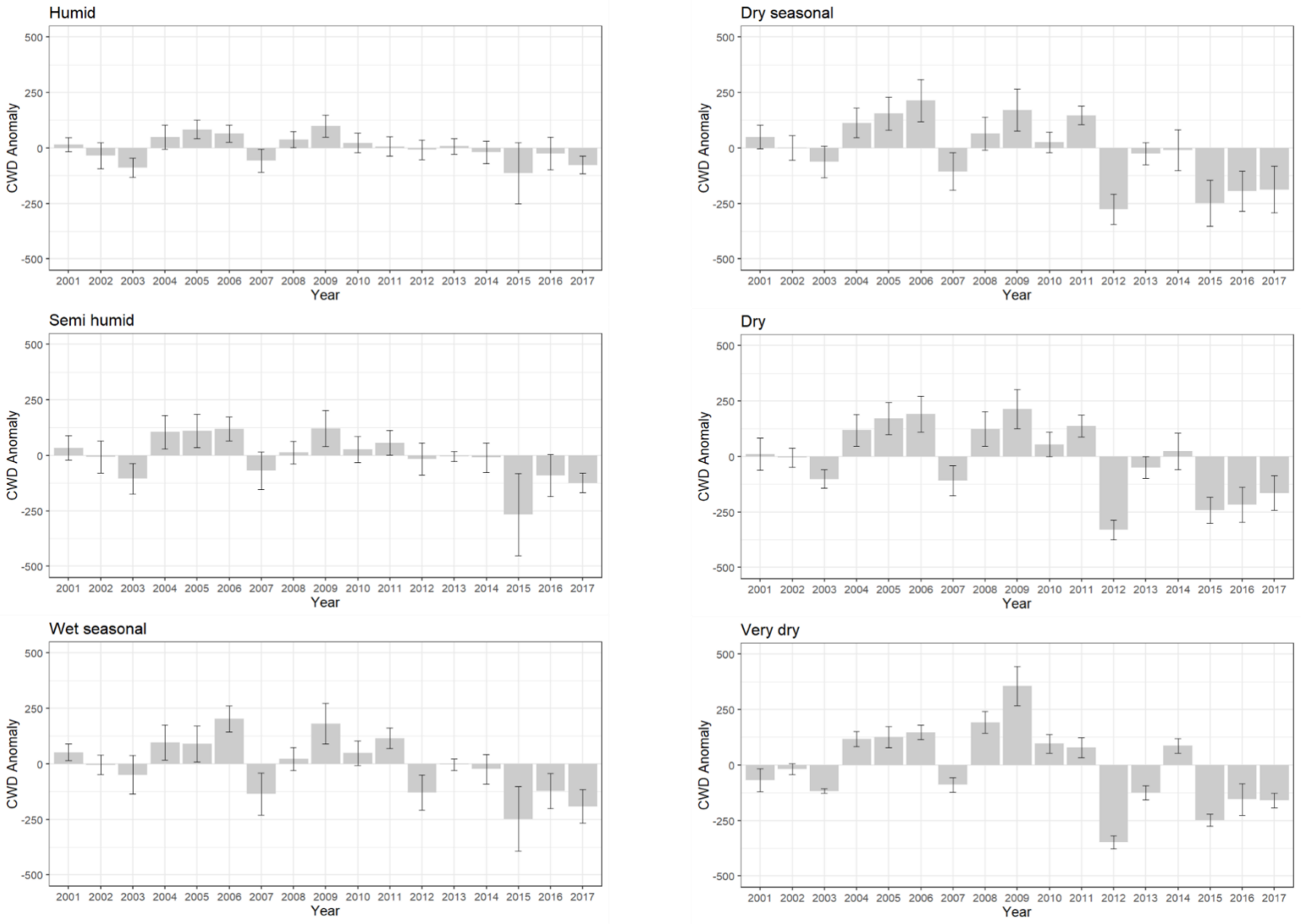

Figure 14: Climatic Water Deficit (CWD) annual anomalies (2001 – 2017) for each Hydroclimatic class. Anomalies were calculated as difference between CWD climatological mean (1958 – 2017) and each year of the analyzed series (2001-2017). In this way, positive values indicate wetter years, and negative values drier years.

Humid

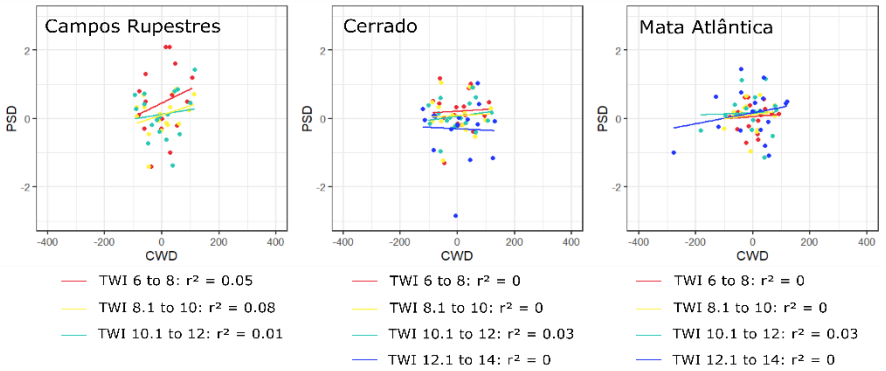

Humid - 1 year lag

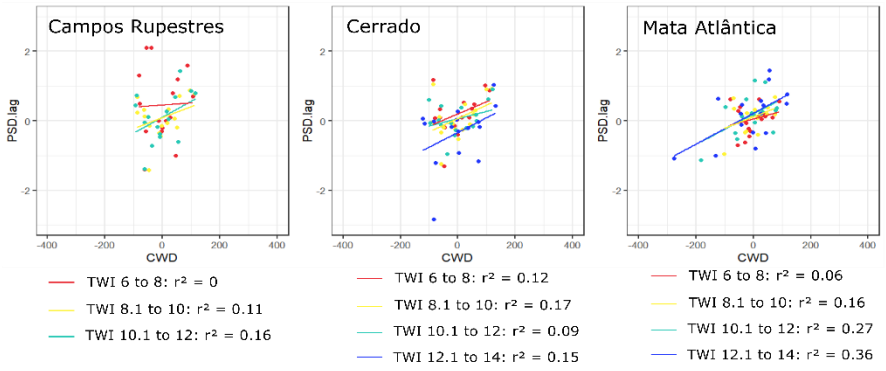

Semi humid

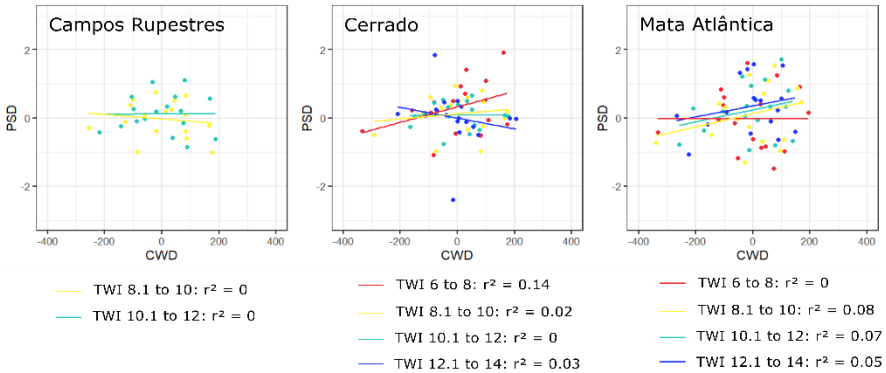

Semi humid - 1 year lag

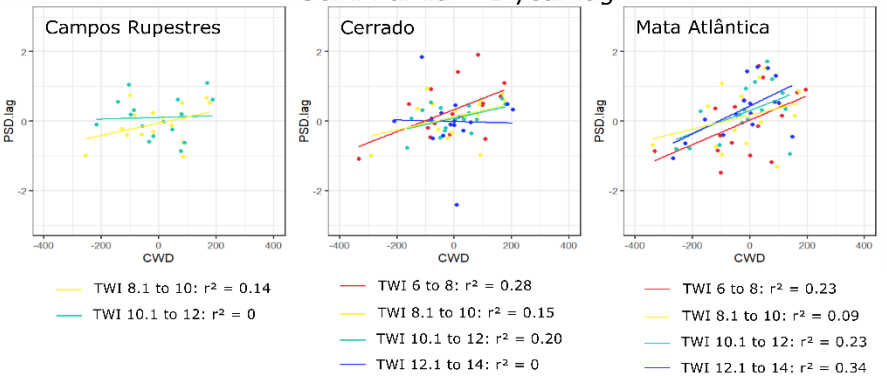

Wet seasonal

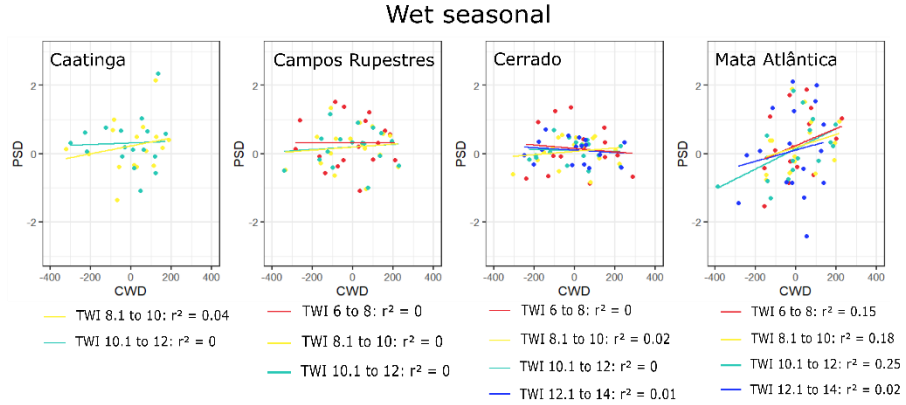

Wet seasonal - 1 year lag

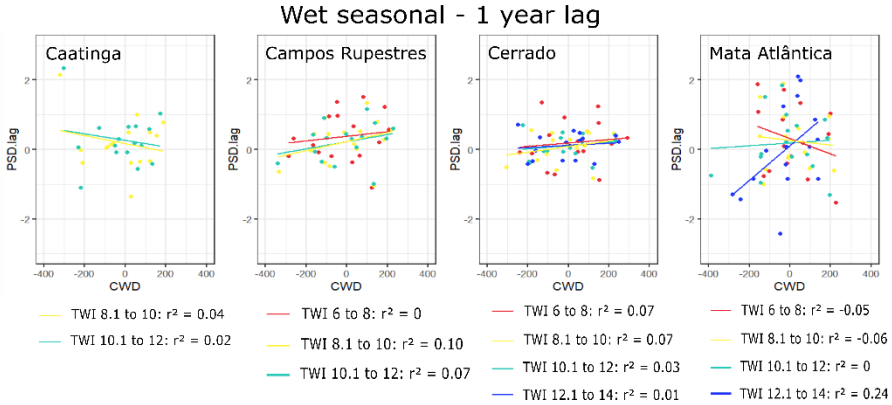

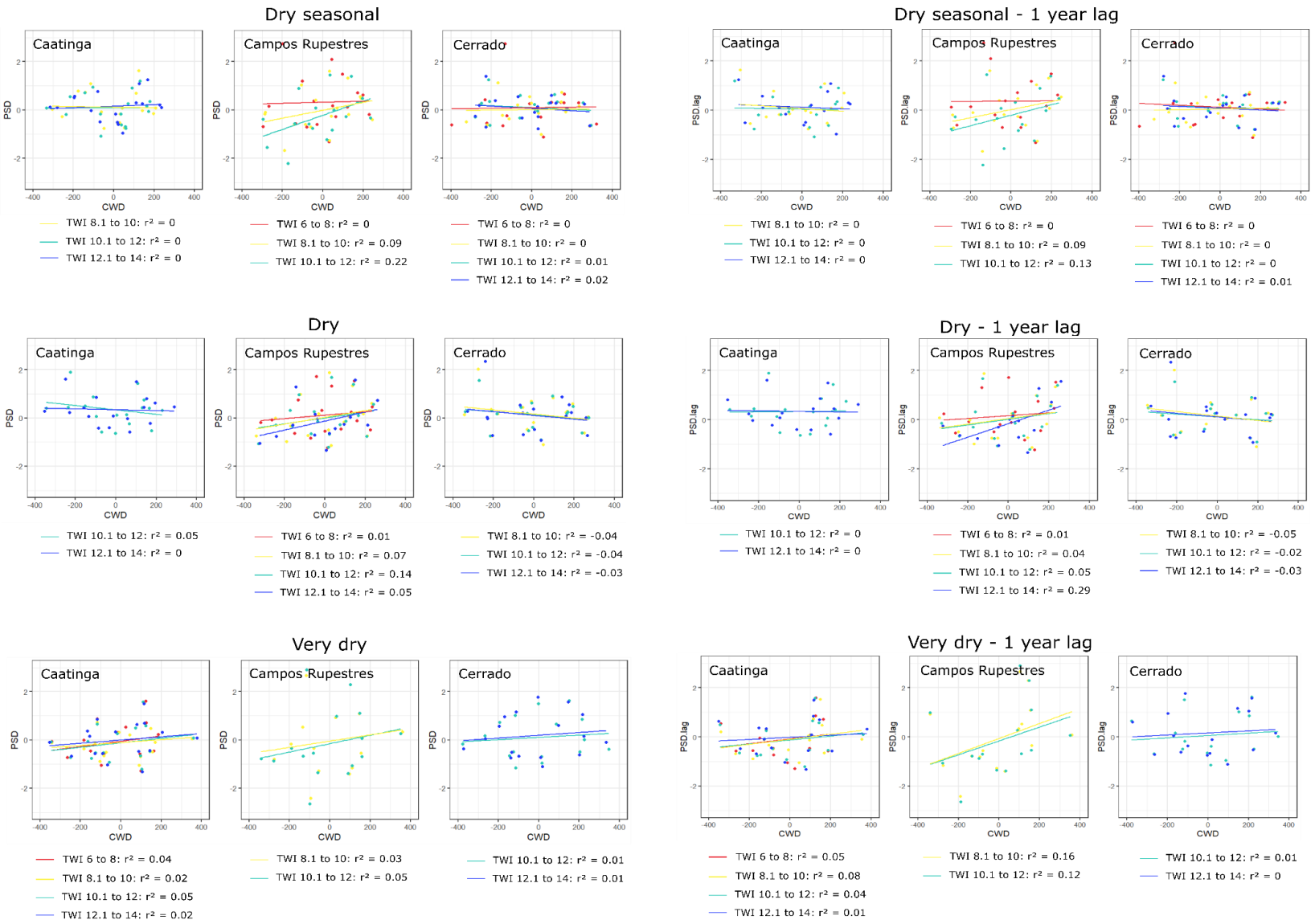

Figure 15: Linear regressions showing the interannual relationship between annual phase shift difference (PSD) (2001 -2017) and the respective annual CWD anomaly (20017-2017) for each hydroclimatic class and each vegetation type analyzed. Linear regressions were adjusted for TWI intervals found for the vegetation type within the hydroclimatic class. Left column indicates the linear regressions for immediate response between phase shift difference and CWD anomaly, while right column indicates the same relationship with a 1-year lag.

5. DISCUSSION

Vegetation types in seasonally dry to dry environments usually have high adaptations to cope with water shortage, being that drought avoidance and drought tolerance are considered the main strategies that plants use to resist to dehydration (Volaire, 2018). We were able to observe these strategies across the Espinhaço Range, which emerged from the contrasting and highly plastic vegetation responses to water availability regarding the hydroclimatic regime experienced.

We observed that the drier or more seasonal a region becomes, the more the vegetation from different biomes may behave functionally more similarly than vegetation of the same biome under different hydrological regimes. This was well captured by the "*Campos Rupestres*" and "*Cerrado*" temporal responses to CWD, being that in drier regimes ("*Dry*" and "*Very dry"*) their responses are similar to those of "*Caatinga*" and in moister regimes ("*Humid"* and "*Semi humid*") they are more similar to "*Mata Atlântica*". This heterogeneity in hydroclimatic and vegetation relationship within a single biome shows that the traditional biome classification may not be an ideal representation of ecosystems function, which agrees previous global scale studies (Moncrieff, Hickler and Higgins, 2015; Higgins, Buitenwerf and Moncrieff, 2016).

In general, wetter climates favors a leaf evergreen habit while dry climates are beneficial to deciduous plants (Vico *et al.*, 2015). The capacity of plants to acclimatize to a variety of environmental conditions and, therefore, to display different strategies to water availability was observed specially to *"Caatinga"*, "*Campos Rupestres*" and "*Cerrado*", while "*Mata Atlântica*" did not show a clear pattern of response, with high variance detected within the monthly coupling values. Despite this simple differentiation between wet and dry climates, we observed that in the

Espinhaço region a much more complex hydroclimatic dynamic overlaps the spatialization of environmental conditions and vegetation strategies to water availability.

While "*Humid*", "*Semi humid*", "*Dry*" and "*Very dry*" regions may favor the establishment of more adapted vegetation to their intra-annual hydroclimatic conditions, transitional regions with high hydroclimatic seasonality such as "*Wet seasonal*" and "*Dry seasonal*" are well suited to harbor different vegetation types with divergent water use strategies. We observed this for all vegetation types since they spanned one ("*Caatinga*" and "*Mata Atlântica*") or both ("*Campos Rupestres*" and "*Cerrado*") transitional hydroclimatic regions, which indicates that hydroclimate seasonality on these environments is not a limiting factor for a vast spectrum of vegetation types, from grasslands to woody plants.

The increasing coupling pattern between NDVI and CWD from wetter to drier regions observed for "*Caatinga*", "*Campos Rupestres*" and "*Cerrado*" shows that the productivity of these vegetation types is influenced by water availability when it is a limiting factor, but when it is not, it may be firstly influenced by other environmental conditions, especially "*Campos Rupestres*" and "*Cerrado*" which spanned all hydroclimatic regions. While vegetation type responses to water availability on the northern region of Espinhaço are closer to "*Caatinga*" strategies, on the southern portion they are much more similar to "*Mata Atlântica*" water availability responses.

In drier regions such as in "*Very dry*" and "*Dry*" classes, water shortage constitutes a selective pressure determining phenological and physiological vegetation strategies (de Lima et al. 2012) highlighting that water is the main abiotic factor controlling vegetation seasonality in these environments (Araújo, Castro and Albuquerque, 2007; Guan *et al.*, 2015). As we observed by the high degree of coupling between CWD and NDVI, "*Caatinga*", "*Campos Rupestres*" and "*Cerrado*" vegetation in these dry regions behave as opportunistic species which flushes its leaves

as water becomes available and shed their leaves to escape from drought, having drought avoidance strategies to periods of low water availability (Reich and Borchert, 1984; Colwell *et al.*, 2008; Vico *et al.*, 2015; Streher *et al.*, 2017).

In wetter regions such as in "*Humid*" and "*Semi humid*" classes, water may not represent a selective pressure on plant productivity. Even experiencing a dry season, the higher volume of rainfall during the wet season and the mild to cold temperatures during the dry season favor higher water availability throughout the year. The higher degree of decoupling between CWD and NDVI in these regions, observed for "*Campos Rupestres*", "*Cerrado*" and "*Mata Atlântica*", indicates that despite their structural differences, they may behave functionally similar as scheduled species, with leaf flush occurring in response to photoperiod or temperature (Vico *et al.*, 2015; Streher *et al.*, 2017).

This similarity between "*Cerrado*" and "*Mata Atlântica*" productivity timing in wetter regions corroborates previous studies on savannas and moist forests relationships, but does not hold for drier regions. Climate is a weaker control on the adjacent distribution of moist forests and savannas when compared to Africa and Australia (Murphy and Bowman, 2012). Furthermore, the evolution of the Brazilian Cerrado is directed linked to historical plant adaptations to recurrent fire events (Simon *et al.*, 2009), which may partially explain their distribution despite sharing the same hydroclimatic regimes.

We did not find topo-edaphic conditions to have major and direct effect on plant distribution and production. The topo-edaphic influences on vegetation distribution and production were restricted to the detected anomalies sites, where the expected relationship of taller vegetation and higher biomass occupying wetter regions and *vice-versa* did not hold. "*Cerrado*" presented two anomalies, A1 and A2, the first where smaller trees and low AGB was found in a region with high water

availability located at the southern Espinhaço highlands. This region with rugged topography suggests that, despite the hydroclimatically favorable conditions, topo-edaphic conditions prevent the establishment of taller vegetation and more carbon allocation. A2 is an example of topo-edaphic conditions overlapping unfavorable hydroclimatic conditions, since the smooth lowlands of the *São Francisco* river favors soil water storage and facilitates plant access to water during the dry season.

A3, where shorter trees and low biomass vegetation are located in regions with high water availability within the "*Humid*" and "*Semi humid*" classes, may have two different explanations. The first is related to the *restinga* coastal vegetation, and the second related to high elevation forests. A4, where we found abnormally low AGB and canopy heights in a region with relatively high AET and medium CWD, is related to the "*Mata Atlântica*" and "*Caatinga*" transition.

Besides the intra-annual coupling of vegetation productivity and water availability analyzed, we conducted an assessment of the interannual variability of this coupling and the role of topography on controlling the responses. The interannual vegetation responses to climate variability is crucial to better understand and predict long-term ecosystem function and stability (Garcia and Ustin, 2001). We found an intensity CWD interannual variability gradient over the study area, with northern regions experiencing greater CWD anomalies than southern regions. "*Caatinga*" NDVI and CWD coupling, which experiences the largest variance on CWD interannual fluctuations, was not responsive to the variability over the years, while the opposite was found to "*Mata Atlântica*".

The variability over the years of vegetation productivity responses to water availability in "*Caatinga*" was not correlated to fluctuations anomalies in CWD. This indicates that despite this biome seasonal productivity being closely controlled by water availability, it is also capable of buffering water availability interannual variability in both directions, wetter or drier years, in order

to maintain its productivity seasonal periodicity. Tropical dry forests production and phenology follows spatial and temporal patterns of water availability, where given the degree of seasonality some species may appear or become dominant (Clary, 2008). In the Caatinga biome, even sites with low species diversity can host communities with complex phenological patterns, this can make the ecosystem hydrologic response relatively stable and maintain constant productivity (Souza *et al.*, 2016).

"*Campos Rupestres*" vegetation seasonal productivity timing was affected by interannual CWD variability in sites of drier hydroclimatic characteristics and topo-edaphic conditions favorable to water accumulation. As said before, "*Campos Rupestres*" productivity is highly influenced by climate given the plasticity of its coupling with CWD over the study area. In moister regions, photoperiod plays a key role on triggering campos rupestres phenological events (Garcia, Barros, And Lemos-Filho 2017), while in drier regions water availability seems to be the main driver. In this way, "*Campos Rupestres*" sites in drier regions, which had higher values of CWD anomalies over the analyzed years, were forced to adapt its seasonal phenological events to cope with the climatic fluctuations, being possible only in sites capable of retaining water (higher TWI). This indicates that topography modulates "*Campos Rupestres*" climatic resilience in drier regions.

In moister region, such as "*Humid*" and "*Semi humid*" classes, "*Cerrado*" and "*Mata Atlântica*" seasonal productivity coupling to water availability were highly sensitive to year-to-year CWD anomalies, with both showing higher responses with a 1-year lag. Aseasonality in humid environments leads to phenological events triggered by other environmental cues than water availability (Reich, 1995), since droughts events are rare and sparse. But in other hand, abnormally interannual changes in water availability may lead to a forcing pressure on these timing of phenological events for these vegetation types (Reich, 1995; Kanniah, Beringer and Hutley, 2013),

as was reported by our results. In addition, since these regions did not experience high anomalies over the years, the cumulative effect of consecutive anomalies showed a better relationship with the vegetation productivity and CWD coupling, expressed by the 1-year lag results for "*Cerrado*" and "*Mata Atlântica*". This indicates, that "*Cerrado*" and "*Mata Atlântica*" in moister regions were capable of tracking interannual variability with the anomalies' magnitudes reported over the years, but that they are also sensitive to changes and may be largely impacted in scenarios of higher and more extreme year-to-year water availability variations.

Given all the points discussed above, we propose a schematic representation of the relationship between vegetation productivity and their responses to both, intra-annual seasonality and inter-annual fluctuations on water availability (Figure 16).

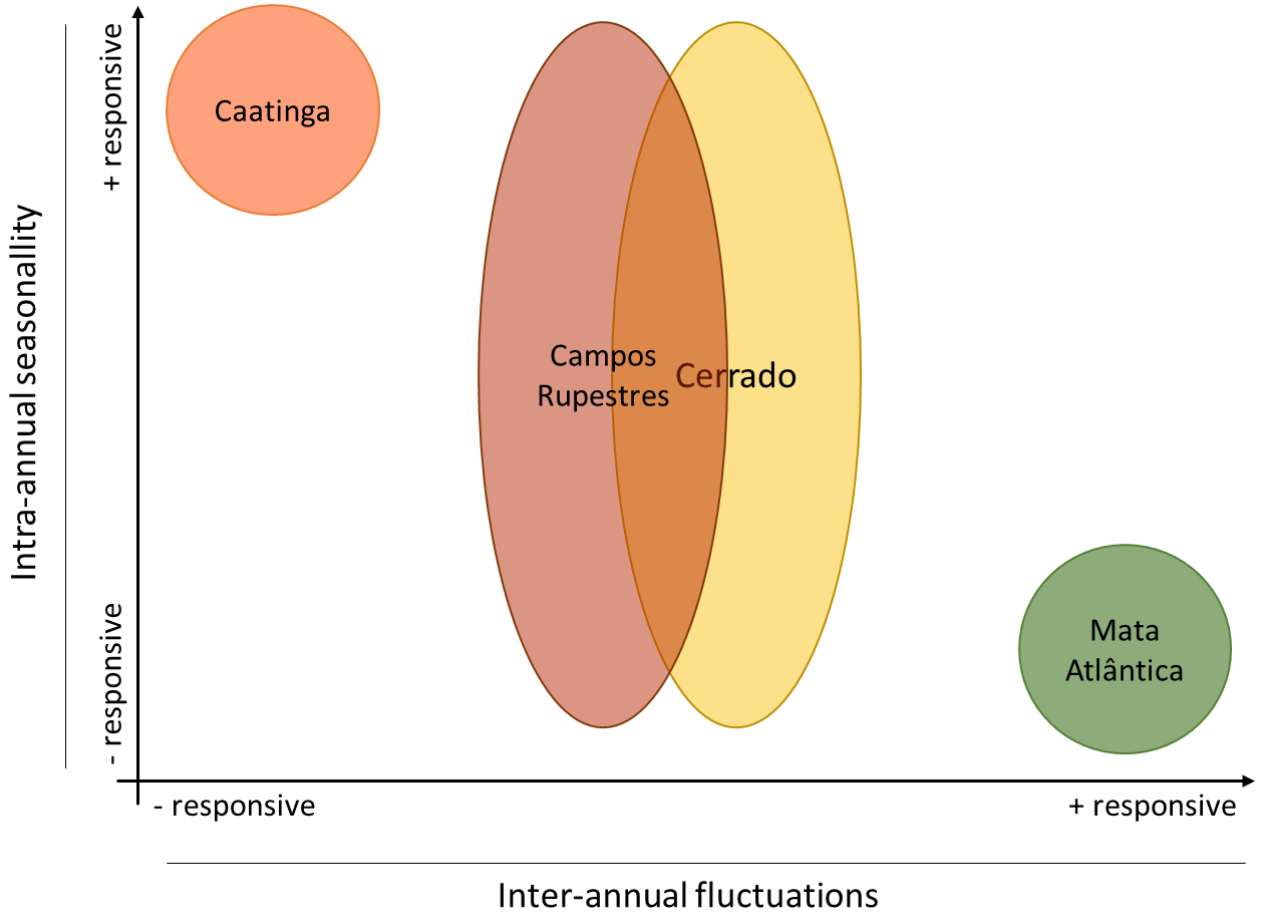

Figure 16: Schematic representation of the relationship between the analyzed vegetation classes productivity to water availability in two temporal dimensions, intra-annual and inter-annual.

6. CONCLUSION

In this study we conclude that in the seasonally dry montane system of the Espinhaço Range, most of the spatio-temporal vegetation productivity dynamics are driven by hydroclimatic and/or topo-edaphic conditions.

Our results show that each vegetation type analyzed across the Espinhaço Range had a different response to water availability. "*Caatinga*" vegetation had a plastic and relatively fast response to CWD and was the most water-constrained vegetation type. "*Cerrado*" and "*Campos Rupestres*" had similar responses to fluctuations in water deficit, showing a gradient of slower to faster responses from "*Humid"* to "*Very dry*" hydroclimatic regions, with "*Cerrado*" experiencing high water deficits during the dry season and, "*Campos Rupestres*" experiencing bothm, water constraints and low evaporative demand as an effect of the high altitudes and lower temperatures.

"*Mata Atlântica*" did not show a clear pattern of responses to seasonality on water availability, with high variance on its NDVI and CWD coupling values, that could have been biased by its highly diverse vegetation types which are classified as a same biome. Our results also show that there is no significant difference in water availability between "*Cerrado*" and "*Mata Atlântica*" regions during the rainy season, and that their main hydroclimatic discrepancies were restricted to small differences in the length of the dry season, and that other environmental conditions may play a more significant role on vegetation dynamics, such as the fire regime and temperature and light availability.

We also found that among all biomes analyzed, "*Cerrado*" and "*Mata Atlântica*" was the most sensitive regarding the CWD interannual variability, especially in sites with moist conditions. Since

over the period assessed those regions did not presented high variability on year-to-year CWD, we argue that more extreme climatic years can have a large impact on the capacity of these vegetation phenology tracking interannual variability. These results have important implications for future studies and modeling of projected climate change, since the assessed ecosystems will be exposed to different responses of their hydrological cycle, therefore, impacting water use strategy and efficiency.

7. REFERENCES

Abatzoglou, J. T. *et al.* (2018) 'TerraClimate, a high-resolution global dataset of monthly climate and climatic water balance from 1958–2015', *Scientific Data*, 5, p. 170191. doi: 10.1038/sdata.2017.191.

Alkmin, F. F. (2012) 'Serra do Espinhaço e Chapada Diamantina', in Hasui, Y. et al. (eds) *A Geologia do Brasil*. São Paulo: Beca, pp. 236–244.

Allan, R. P. and Soden, B. J. (2008) 'Atmospheric Warming and the Amplification of Precipitation Extremes', *Science*, 321(5895), pp. 1481–1484. doi: 10.1126/science.1160787.

Allen, K. *et al.* (2017) 'Will seasonally dry tropical forests be sensitive or resistant to future changes in rainfall regimes?', *Environmental Research Letters*, 12(2), p. 023001. doi: 10.1088/1748-9326/aa5968.

Allen, R. G. *et al.* (1998) 'Crop evapotranspiration - Guidelines for computing crop water requirements - FAO Irrigation and drainage paper 56 By', pp. 1–15.

Aparecido, L. M. T. *et al.* (2018) 'Ecohydrological drivers of Neotropical vegetation in montane ecosystems', *Ecohydrology*, (February 2017), p. e1932. doi: 10.1002/eco.1932.

Araújo, E. L., Castro, C. C. and Albuquerque, U. P. (2007) 'Dynamics of Brazilian Caatinga – A Review Concerning the Plants , Environment and People', *Functional Ecosystems and Communities*, 1(October 2015), pp. 15–28. doi: 10.1111/1365-2745.12712.

Austin, M. P. and Van Niel, K. P. (2011) 'Improving species distribution models for climate change studies: variable selection and scale', *Journal of Biogeography*, 38(1), pp. 1–8. doi: 10.1111/j.1365-2699.2010.02416.x.

Avitabile, V. *et al.* (2016) 'An integrated pan-tropical biomass map using multiple reference datasets', *Global Change Biology*, 22(4), pp. 1406–1420. doi: 10.1111/gcb.13139.

Baik, J. and Choi, M. (2015) 'Evaluation of remotely sensed actual evapotranspiration products from COMS and MODIS at two different flux tower sites in Korea', *International Journal of Remote Sensing*, 36(1), pp. 375–402. doi: 10.1080/01431161.2014.998349.

Beck, P. S. A. and Goetz, S. J. (2011) 'Satellite observations of high northern latitude vegetation productivity changes between 1982 and 2008: ecological variability and regional differences', *Environmental Research Letters*, 6(4). doi: 10.1088/1748-9326/7/2/029501.

Bencke, C. C. and Morellato, L. P. C. (2002) 'Estudo comparativo da fenologia de nove espécies arbóreas em três tipos de floresta atlântica no sudeste do Brasil', *Revista Brasileira de Botânica*, 25(2), pp. 237–248. doi: 10.1590/S0100-84042002000200012.

Benites, V. M. *et al.* (2007) 'Soils associated with rock outcrops in the Brazilian mountain ranges Mantiqueira and

Espinhaço', *Revista Brasileira de Botânica*, 30(4), pp. 569–577. doi: 10.1590/S0100-84042007000400003.

Bohner, J. and Selige, T. (2002) 'SPATIAL PREDICTION OF SOIL ATTRIBUTES USING TERRAIN ANALYSIS AND CLIMATE REGIONALISATION'.

Bonan (2016) *Ecological Climatology*. Cambridge: Cambridge University Press. doi: 10.1017/CBO9781107339200.

Busetto, L. and Ranghetti, L. (2016) 'MODIStsp: An R package for automatic preprocessing of MODIS Land Products time series', *Computers and Geosciences*. Elsevier, 97, pp. 40–48. doi: 10.1016/j.cageo.2016.08.020.

de Camargo, M. G. G. *et al.* (2018) 'Leafing patterns and leaf exchange strategies of a cerrado woody community', *Biotropica*, 50(3), pp. 442–454. doi: 10.1111/btp.12552.

Chambers, L. E. *et al.* (2013) 'Phenological Changes in the Southern Hemisphere', *PLoS ONE*, 8(10). doi: 10.1371/journal.pone.0075514.

Clary, J. (2008) 'Rainfall seasonality determines annual/perennial grass balance in vegetation of Mediterranean Iberian', *Plant Ecology*, 195(1), pp. 13–20. doi: 10.1007/s11258-007-9294-9.

Colwell, R. K. *et al.* (2008) 'Global Warming, Elevational Range Shifts, and Lowland Biotic Attrition in the Wet Tropics', *Science*, 322(5899), pp. 258–261. doi: 10.1126/science.1162547.

Didan, K. (2015) 'MOD13A3 MODIS/Terra vegetation Indices Monthly L3 Global 1km SIN Grid V006 [Data set]', *NASA EOSDIS LP DAAC*, 2015(June). doi: 10.5067/MODIS/MOD13A3.006.

Dilts, T. E. *et al.* (2015) 'Functionally relevant climate variables for arid lands: a climatic water deficit approach for modelling desert shrub distributions', *Journal of Biogeography*, 42(10), pp. 1986–1997. doi: 10.1111/jbi.12561.

Domec, J.-C. *et al.* (2010) 'Hydraulic redistribution of soil water by roots affects whole-stand evapotranspiration and net ecosystem carbon exchange', *New Phytologist*, 187(1), pp. 171–183. doi: 10.1111/j.1469-8137.2010.03245.x.

Elsen, P. R. and Tingley, M. W. (2015) 'Global mountain topography and the fate of montane species under climate change', *Nature Climate Change*, 5(8), pp. 772–776. doi: 10.1038/nclimate2656.

Fekete, B. M., Pisacane, G. and Wisser, D. (2016) 'Crystal balls into the future: are global circulation and water balance models ready?', *Proceedings of the International Association of Hydrological Sciences*, 374, pp. 41–51. doi: 10.5194/piahs-374-41-2016.

Fenner, M. (1998) 'The phenology of growth and reproduction in plants', *Perspectives in Plant Ecology, Evolution and Systematics*, 1(1), pp. 78–91. doi: 10.1078/1433-8319-00053.

Fernandes, G. W. (2016) *Ecology and Conservation of Mountaintop grasslands in Brazil*. Edited by G. W. Fernandes. Cham: Springer International Publishing. doi: 10.1007/978-3-319-29808-5.

Frank, D. C. *et al.* (2015) 'Water-use efficiency and transpiration across European forests during the Anthropocene', *Nature Climate Change*, 5(6), pp. 579–583. doi: 10.1038/nclimate2614.

Funk, C. *et al.* (2015) 'The climate hazards infrared precipitation with stations—a new environmental record for monitoring extremes', *Scientific Data*, 2, p. 150066. doi: 10.1038/sdata.2015.66.

Galvão, L. S. *et al.* (2016) 'Investigation of terrain illumination effects on vegetation indices and VI-derived phenological metrics in subtropical deciduous forests', *GIScience & Remote Sensing*, 53(3), pp. 360–381. doi: 10.1080/15481603.2015.1134140.

GARCIA, L. C., BARROS, F. V. and LEMOS-FILHO, J. P. (2017) 'Environmental drivers on leaf phenology of ironstone outcrops species under seasonal climate', *Anais da Academia Brasileira de Ciências*, 89(1), pp. 131–143. doi: 10.1590/0001-3765201720150049.

Garcia, M. and Ustin, S. L. (2001) 'Detection of interannual vegetation responses to climatic variability using AVIRIS data in a coastal savanna in California', *IEEE Transactions on Geoscience and Remote Sensing*, 39(7), pp. 1480–1490. doi: 10.1109/36.934079.

Graham, C. H. *et al.* (2014) 'The origin and maintenance of montane diversity: Integrating evolutionary and ecological processes', *Ecography*, 37(8), pp. 711–719. doi: 10.1111/ecog.00578.

Guan, K. *et al.* (2015) 'Photosynthetic seasonality of global tropical forests constrained by hydroclimate', *Nature Geoscience*, 8(4), pp. 284–289. doi: 10.1038/ngeo2382.

Hawkins, B. A. *et al.* (2003) 'ENERGY, WATER, AND BROAD-SCALE GEOGRAPHIC PATTERNS OF SPECIES RICHNESS', *Ecology*, 84(12), pp. 3105–3117. doi: 10.1890/03-8006.

Higgins, S. I., Buitenwerf, R. and Moncrieff, G. R. (2016) 'Defining functional biomes and monitoring their change globally', *Global Change Biology*, 22(11), pp. 3583–3593. doi: 10.1111/gcb.13367.

Hijmans, R. J. (2017) 'Introduction to the ' raster ' package (version 2 . 6-7)', (2008).

Hopper, S. D. (2009) 'OCBIL theory: towards an integrated understanding of the evolution, ecology and conservation of biodiversity on old, climatically buffered, infertile landscapes', *Plant and Soil*, 322(1–2), pp. 49–86. doi: 10.1007/s11104-009-0068-0.

Jones, M. O., Kimball, J. S. and Nemani, R. R. (2014) 'Asynchronous Amazon forest canopy phenology indicates adaptation to both water and light availability', *Environmental Research Letters*. IOP Publishing, 9(12), p. 124021. doi: 10.1088/1748-9326/9/12/124021.

Kane, V. R. *et al.* (2015) 'Water balance and topography predict fire and forest structure patterns', *Forest Ecology and Management*. Elsevier B.V., 338, pp. 1–13. doi: 10.1016/j.foreco.2014.10.038.

Kanniah, K. D., Beringer, J. and Hutley, L. B. (2013) 'Response of savanna gross primary productivity to interannual variability in rainfall', *Progress in Physical Geography: Earth and Environment*, 37(5), pp. 642–663. doi: 10.1177/0309133313490006.

Kohler, T. and Maselli, D. (2012) *Mountains and Climate Change*. Available at: www.mountainpartnership.org%5Cnwww.cde.unibe.ch.

Körner, C. *et al.* (2017) 'A global inventory of mountains for bio-geographical applications', *Alpine Botany*, 127(1), pp. 1–15. doi: 10.1007/s00035-016-0182-6.

Krishnaswamy, J., John, R. and Joseph, S. (2014) 'Consistent response of vegetation dynamics to recent climate change in tropical mountain regions', *Global Change Biology*, 20(1), pp. 203–215. doi: 10.1111/gcb.12362.

LIU, H.-J. *et al.* (2009) 'Quantitative Analysis of Moisture Effect on Black Soil Reflectance', *Pedosphere*. Soil Science Society of China, 19(4), pp. 532–540. doi: 10.1016/S1002-0160(09)60146-6.

Lopes, A. P. *et al.* (2016) 'Leaf flush drives dry season green-up of the Central Amazon', *Remote Sensing of Environment*. Elsevier Inc., 182, pp. 90–98. doi: 10.1016/j.rse.2016.05.009.

Lutz, J. A., van Wagtendonk, J. W. and Franklin, J. F. (2010) 'Climatic water deficit, tree species ranges, and climate change in Yosemite National Park', *Journal of Biogeography*, 37(5), pp. 936–950. doi: 10.1111/j.1365-2699.2009.02268.x.

McIntyre, P. J. *et al.* (2015) 'Twentieth-century shifts in forest structure in California: Denser forests, smaller trees, and increased dominance of oaks', *Proceedings of the National Academy of Sciences*, 112(5), pp. 1458–1463. doi: 10.1073/pnas.1410186112.

McLaughlin, B. *et al.* (2017) 'Hydrologic refugia, plants and climate change', *Global Change Biology*, 23, pp. 000–000. doi: 10.1111/gcb.13629.

Meinzer, F. C. *et al.* (2004) 'Converging patterns of uptake and hydraulic redistribution of soil water in contrasting woody vegetation types', *Tree Physiology*, 24(8), pp. 919–928. doi: 10.1093/treephys/24.8.919.

Meybeck, A. M., Green, P. and Vörösmarty, C. (2001) 'A New Typology for Mountains and Other Relief Classes A New Typology for Mountains and Other Relief Classes', *Mountain Research and Development*, 21(May), pp. 34–45. doi: 10.1659/0276-4741(2001) 021[0034:ANTFMA]2.0.CO;2.

Mod, H. K. *et al.* (2016) 'What we use is not what we know: environmental predictors in plant distribution models', *Journal of Vegetation Science*, 27(6), pp. 1308–1322. doi: 10.1111/jvs.12444.

Moncrieff, G. R., Hickler, T. and Higgins, S. I. (2015) 'Intercontinental divergence in the climate envelope of major plant biomes', *Global Ecology and Biogeography*, 24(3), pp. 324–334. doi: 10.1111/geb.12257.

Morellato, L. P. C. *et al.* (2000) 'Phenology of Atlantic Rain Forest Trees: A Comparative Study1', *Biotropica*, 32(4b), pp. 811–823. doi: 10.1111/j.1744-7429.2000.tb00620.x.

Murphy, B. P. and Bowman, D. M. J. S. (2012) 'What controls the distribution of tropical forest and savanna?', *Ecology Letters*, 15(7), pp. 748–758. doi: 10.1111/j.1461-0248.2012.01771.x.

Myers, N. *et al.* (2000) 'Biodiversity hotspots for conservation priorities', *Nature*, 403(6772), pp. 853–858. doi: 10.1038/35002501.

Neumann, R. B. and Cardon, Z. G. (2012) 'The magnitude of hydraulic redistribution by plant roots: a review and synthesis of empirical and modeling studies', *New Phytologist*, 194(2), pp. 337–352. doi: 10.1111/j.1469-8137.2012.04088.x.

Oliveira, R. S. *et al.* (2014) 'The hydroclimatic and ecophysiological basis of cloud forest distributions under current and projected climates', *Annals of Botany*, 113(6), pp. 909–920. doi: 10.1093/aob/mcu060.

Pepin, N. *et al.* (2015) 'Elevation-dependent warming in mountain regions of the world', *Nature Climate Change*, 5(5), pp. 424–430. doi: 10.1038/nclimate2563.

Pettorelli, N. *et al.* (2005) 'Using the satellite-derived NDVI to assess ecological responses to environmental change', *Trends in Ecology & Evolution*, 20(9), pp. 503–510. doi: 10.1016/j.tree.2005.05.011.

Portillo-Quintero, C. A. and Sánchez-Azofeifa, G. A. (2010) 'Extent and conservation of tropical dry forests in the Americas', *Biological Conservation*. Elsevier Ltd, 143(1), pp. 144–155. doi: 10.1016/j.biocon.2009.09.020.

Quesada, C. A. *et al.* (2008) 'Seasonal variations in soil water in two woodland savannas of central Brazil with different fire histories', *Tree Physiology* , 28(3), pp. 405–415. doi: 10.1093/treephys/28.3.405.

R Core Team (2013) 'R: A language and environment for statistical computing', *R Foundation for Statistical Computing, Vienna, Austria*, 0, p. 62. doi: 10.1016/0164-1212(87)90019-7.

Rangwala, I. and Miller, J. R. (2012) 'Climate change in mountains: A review of elevation-dependent warming and its possible causes', *Climatic Change*, 114(3–4), pp. 527–547. doi: 10.1007/s10584-012-0419-3.

Rapini, A. *et al.* (2008) 'A flora dos campos rupestres da Cadeia do Espinhaço', *Megadiversidade*, 4(1–2), pp. 16–24. Available at: http://www.inot.org.br/artigo/Rapini_et_al_2008_A_flora_dos_campos_rupestres_da_Cadeia_do_Espinhaco.pdf.

Reich, P. B. (1995) 'Phenology of tropical forests: patterns, causes, and consequences1', *Canada Journal of Botany*, 73(August 1993), pp. 164–174. doi: 10.1139/b95-020.

Reich, P. B. and Borchert, R. (1984) 'Water Stress and Tree Phenology in a Tropical Dry Forest in the Lowlands of Costa Rica', *The Journal of Ecology*, 72(1), p. 61. doi: 10.2307/2260006.

Ribeiro, K. T. *et al.* (2009) 'Aferição dos limites da Mata Atlântica na Serra do Cipó, MG, Brasil, visando maior compreensão e proteção de um mosaico vegetacional fortemente ameaçado', *Natureza & Conservação*, 7(1), pp. 30–49.

Santos, M. F., Serafim, H. and Sano, P. T. (2011) 'Fisionomia e composição da vegetação florestal na Serra do Cipó, MG, Brasil', *Acta Botanica Brasilica*, 25(4), pp. 793–814. doi: 10.1590/S0102-33062011000400007.

Schaefer, C. E. *et al.* (2016) 'The Physical Environment of Rupestrian Grasslands (Campos Rupestres) in Brazil: Geological, Geomorphological and Pedological Characteristics, and Interplays', in *Ecology and Conservation of Mountaintop grasslands in Brazil*. Springer International Publishing.

Schwinning, S. *et al.* (2004) 'Thresholds, memory, and seasonality: Understanding pulse dynamics in arid/semi-arid

ecosystems', *Oecologia*, 141(2), pp. 191–193. doi: 10.1007/s00442-004-1683-3.

Silveira, F. A. O. *et al.* (2016) 'Ecology and evolution of plant diversity in the endangered campo rupestre: a neglected conservation priority', *Plant and Soil*. Plant and Soil, 403(1–2), pp. 129–152. doi: 10.1007/s11104-015-2637-8.

Simon, M. F. *et al.* (2009) 'Recent assembly of the Cerrado, a neotropical plant diversity hotspot, by in situ evolution of adaptations to fire.', *Proceedings of the National Academy of Sciences of the United States of America*, 106(48), pp. 20359–20364. doi: 10.1073/pnas.0903410106.

SOBREIRO, J. F. F. (2015) 'Avaliação Multi-Escala do Regime de Precipitação da Cadeia do Espinhaço Meridional (Brasil)', p. 6.

Sobreiro, J. F. F., Streher, A. S. and Silva, T. S. F. (2017) 'Padrões climáticos e implicações ecológicas em um ambiente montanhoso tropical: análise da Cadeia do Espinhaço meridional (Brasil)', in Gherardi, D. F. M. and Aragão, L. E. O. C. (eds) *Simpósio Brasileiro de Sensoriamento Remoto*. Santos - SP, pp. 7883–7890.

Souza, R. *et al.* (2016) 'Vegetation response to rainfall seasonality and interannual variability in tropical dry forests', *Hydrological Processes*, 30(20), pp. 3583–3595. doi: 10.1002/hyp.10953.

Steinbauer, M. J. *et al.* (2016) 'Topography-driven isolation, speciation and a global increase of endemism with elevation', *Global Ecology and Biogeography*, 25(9), pp. 1097–1107. doi: 10.1111/geb.12469.

Stephenson, N. (1998) 'Actual evapotranspiration and deficit: biologically meaningful correlates of vegetation distribution across spatial scales', *Journal of Biogeography*, 25(5), pp. 855–870. doi: 10.1046/j.1365-2699.1998.00233.x.

Stephenson, N. L. (1990) 'Climatic Control of Vegetation Distribution : The Role of the Water Balance Author (s): Nathan L . Stephenson Source : The American Naturalist , Vol . 135 , No . 5 (May , 1990), pp . 649-670 Published by : The University of Chicago Press for The Ameri', 135(5), pp. 649–670.

Stephenson, N. L. (1990) 'Climatic Control of Vegetation Distribution: The Role of the Water Balance', *The American Naturalist*, 135(5), pp. 649–670. doi: 10.1086/285067.

Streher, A. S. *et al.* (2017) 'Land Surface Phenology in the Tropics: The Role of Climate and Topography in a Snow-Free Mountain', *Ecosystems*. doi: 10.1007/s10021-017-0123-2.

Title, P. O. and Bemmels, J. B. (2018) 'ENVIREM: an expanded set of bioclimatic and topographic variables increases flexibility and improves performance of ecological niche modeling', *Ecography*, 41(2), pp. 291–307. doi: 10.1111/ecog.02880.

Velpuri, N. M. *et al.* (2013) 'A comprehensive evaluation of two MODIS evapotranspiration products over the conterminous United States: Using point and gridded FLUXNET and water balance ET', *Remote Sensing of Environment*, 139, pp. 35–49. doi: 10.1016/j.rse.2013.07.013.

Vico, G. *et al.* (2015) 'Climatic, ecophysiological, and phenological controls on plant ecohydrological strategies in seasonally dry ecosystems', *Ecohydrology*, 8(4), pp. 660–681. doi: 10.1002/eco.1533.

Viviroli, D. *et al.* (2007) 'Mountains of the world, water towers for humanity: Typology, mapping, and global significance', *Water Resources Research*, 43(7), pp. 1–13. doi: 10.1029/2006WR005653.

Volaire, F. (2018) 'A unified framework of plant adaptive strategies to drought: Crossing scales and disciplines', *Global Change Biology*, 24(7), pp. 2929–2938. doi: 10.1111/gcb.14062.

Wagstaff, K. *et al.* (2001) 'Constrained K-means Clustering with Background Knowledge', *International Conference on Machine Learning*, pp. 577–584. doi: 10.1109/TPAMI.2002.1017616.

Wang-Erlandsson, L. *et al.* (2016) 'Global root zone storage capacity from satellite-based evaporation', *Hydrology and Earth System Sciences*, 20(4), pp. 1459–1481. doi: 10.5194/hess-20-1459-2016.

WELTZIN, J. F. *et al.* (2003) 'Assessing the Response of Terrestrial Ecosystems to Potential Changes in Precipitation', *BioScience*, 53(10), p. 941. doi: 10.1641/0006-3568(2003)053[0941:ATROTE]2.0.CO;2.

8. SUPPLEMENTARY MATERIAL

IMPROVING THE CHOICE OF HYDROCLIMATIC VARIABLES FOR MODELING VEGETATION RESPONSES TO MOISTURE IN THE ESPINHAÇO RANGE (BRAZIL)

João Francisco Ferreira Sobreiro[1], Annia Susin Streher[2], Thiago Sanna Freire Silva[3]

[1] Universidade Estadual Paulista (UNESP), Instituto de Geociências e Ciências Exatas, Rio Claro, jffsobreiro@gmail.com;

[2] Universidade Estadual Paulista (UNESP), Instituto de Biociências, Rio Claro, annia.streher@gmail.com;

[3] Universidade Estadual Paulista (UNESP), Instituto de Geociências e Ciências Exatas, Rio Claro, thiago.sf.silva@unesp.

ABSTRACT

The capacity of ecological models to better capture and predict ecosystems variations and changes is dependent on the choice of its environmental inputs' variables, being precipitation the mostly used hydroclimatic variable. Yet, water available to plants is a function of rainfall and atmospheric evaporative demand. We assessed which hydroclimatic variable better explains variations in vegetation productivity in a seasonally dry tropical mountain system. We modeled NDVI temporal responses of different vegetation types to Climatic Water Deficit (CWD) and Precipitation, answering the following questions*:* 1) Are the responses of vegetation to different hydroclimatic variables specific for each vegetation type? 2) If so, which hydroclimatic variable better explains vegetation productivity for each vegetation type? We found that seasonally dry vegetation types were more responsive to CWD, while moist vegetation productivity was poorly explained by all hydroclimatic variables. The timing of responses of vegetation to CWD or precipitation varied according to site specificity.

Key words **—** Evapotranspiration, Climatic Water Deficit, Mountain, NDVI, Vegetation productivity.

1. INTRODUCTION

In ecological studies, the identification of environmental variables that are ecophysiologically meaningful is crucial to improve models and better forecast ecosystem changes (Austin and Van Niel, 2011). Hydrological dynamics are a major driver of ecosystem function, and yet, are usually oversimplified when studying species distribution and vegetation dynamics (Mod *et al.*, 2016). Given the importance of water to ecological processes, the choice of predictive hydrological variable is directly related to the capacity of models to capture and predict ecosystem dynamics (Hawkins *et al.*, 2003).

Precipitation is frequently used as a predictor of plant water availability, but it is known that the water available to plants is a function not only of rainfall input, but of a set of other variables, such as atmospheric energy balance (Stephenson, 1998). Stephenson (1998) advocates that many correlative studies on vegetation distribution and water availability do not make use of hydroclimatic parameters that are truly meaningful to plant physiology, and propose that Actual Evapotranspiration (AET) and Climatic Water Deficit (CWD) should be used instead of precipitation, since both variables provide a reasonable biological interpretation, and have shown good correlation with the distribution of different vegetation types, from local to continental scales (Dilts *et al.*, 2015). Both CWD and AET estimate the length and magnitude of hydroclimatic conditions to plants; CWD is related to drought, and AET represents favorable conditions of availability for biologically usable water and energy inputs to the environment (Stephenson, 1998).

In the tropics, vast areas experience seasonally dry climates, which are well-defined by a wet season during which most of the annual precipitation occurs, followed by a prolonged dry season. These areas harbor a great variety of vegetation types, from semi-deciduous to dry forests and savannas (Allen *et al.*, 2017). Seasonally dry tropical environments are expected to experience future changes in periodicity due to climate change, with stronger impacts predicted for higher elevations (Aparecido *et al.*, 2018). Among other impacts, tropical montane ecosystems will potentially suffer an acceleration of their hydrological regimes, caused by an increase on the variability of precipitation patterns (Allan and Soden, 2008), leading to, among others effects, changes in ecosystem functioning and productivity, or improvement of environmental conditions to invasive species, increasing mortality rates and, therefore impacting species diversity and distribution. For this reason, understanding and quantifying the spatial and temporal patterns of seasonal plant water

use can provide important insights on how tropical mountainous ecosystems will respond to climate change.

The Espinhaço Range is a seasonally dry mountainous region feeding the watersheds of three large river basins in Brazil (*São Francisco, Atlântico Leste and Atlântico Sul)*, with a primary S-N direction. This region is an ecotone of semi-deciduous moist forests, savannas, dry forests and mountain vegetation (Figure 1). This ancient landscape, dating back to 640 Mya, has ample topographic and altitudinal variation, with mountain peaks reaching over 2000 meters *a.s.l* (Schaefer *et al.*, 2016). A recent analysis of spatial precipitation patterns in the Espinhaço Range showed that there is no significant difference in total annual rainfall between eastern and western sides, which are occupied by semi-deciduous forest and savanna vegetation, respectively (Streher *et al.*, 2017). For this reason, here we propose an analysis to assess which hydroclimatic variables better explain vegetation dynamics in the Espinhaço Range.

To understand the relations between vegetation productivity and hydroclimatic variables in this tropical mountainous system, and improve variables choice for bioclimatic studies, we addressed the following questions: 1) Are the responses of vegetation to different hydroclimatic variables specific for each vegetation type? 2) If so, which hydroclimatic variable better explains vegetation productivity for each vegetation type?

2. MATERIAL AND METHODS

We adjusted pixel-wise linear regression models between an NDVI dataset, a proxy of vegetation productivity, and two layers of hydroclimatic variables (precipitation and CWD) to assess the temporal vegetation responses to water availability. The linear regression models were fitted using monthly pairwise observations, with 0, 1 and 2-month lags for precipitation and CWD, to capture possible lagged vegetation responses to climate. All datasets covered the period between

January/2001 and December/2017, at monthly intervals, with a 1 x 1 km spatial resolution. To ensure we were sampling natural vegetation, we fitted the models to all pixels within the studied region to reveal broad spatial patterns, but then evaluated model fit only for regions corresponding to known protected areas within the Espinhaço Range.

Vegetation types at each protected area were classified following the Brazilian official biome classification, and then attributed to the protected areas. To delineate the "Campos Rupestres" classification, which is not an official biome, we identified all protected areas that overlaid the Silveira et. al (2016) "Campos Rupestres" delineation, and reclassified it as "Campos Rupestres" protected areas. The vegetation types found on the study area are, hereafter, classified as "Caatinga" (5014 pixels), "Campos Rupestres" (8041 pixels), "Cerrado" (7900 pixels) and "Mata Atlântica" (11572 pixels).

We used a time-series of NDVI images generated from Moderate Resolution Imaging Spectroradiometer (MODIS) images. Data was obtained from the Land Process Distributed Active Archive Center (LP-DAAC – USGS/NASA). Monthly NDVI pixels values result from the best pixel composite of two 16-day composite periods. To improve the quality of pixels, and minimize atmospheric and cloud effects, the 16-day period algorithm chooses the best available pixel within all the acquisition dates. All monthly images were downloaded, mosaiced and transformed to GeoTIFF format using the "MODIStsp" package of the R programming language (Busetto and Ranghetti, 2016).

Precipitation was obtained from the Climate Hazards Infrared Precipitation with Stations (CHIRPS) dataset (Funk *et al.*, 2015). CHIRPS is a quasi-global precipitation dataset which incorporates satellite data of cold cloud duration and gauge stations. Using an interpolation

approach between cold cloud duration rainfall estimates and gauge station data, CHIRPS provides daily, pentadal, monthly, 2 and 3 months aggregated and annual precipitation gridded datasets at a 5 x 5 km spatial resolution. We disaggregated the data to 1 x 1 km spatial resolution to match the NDVI dataset. CHIRPS is freely available at http://chg.geog.ucsb.edu/data/chirps/.

We used the TerraClimate dataset (Abatzoglou *et al.*, 2018) to obtain CWD values, which are gridded (~ 4km) monthly data products. TerraClimate products are generated from the interpolation of different global weather station databases from WorldClim (version 1.4 and version 2.0), CRU Ts4.0 and JRA-55. To calculate AET and CWD, TerraClimate uses a one-dimensional modified Thornthwaite-Mather climatic water-balance model, with CWD given as the difference between Potential Evapotranspiration (PET) and Actual Evapotranspiration (AET). We also disaggregated the data to 1 x 1 km spatial resolution to match thr NDVI dataset. TerraClimate is freely available at http://climatologylab.org/terraclimate.html.

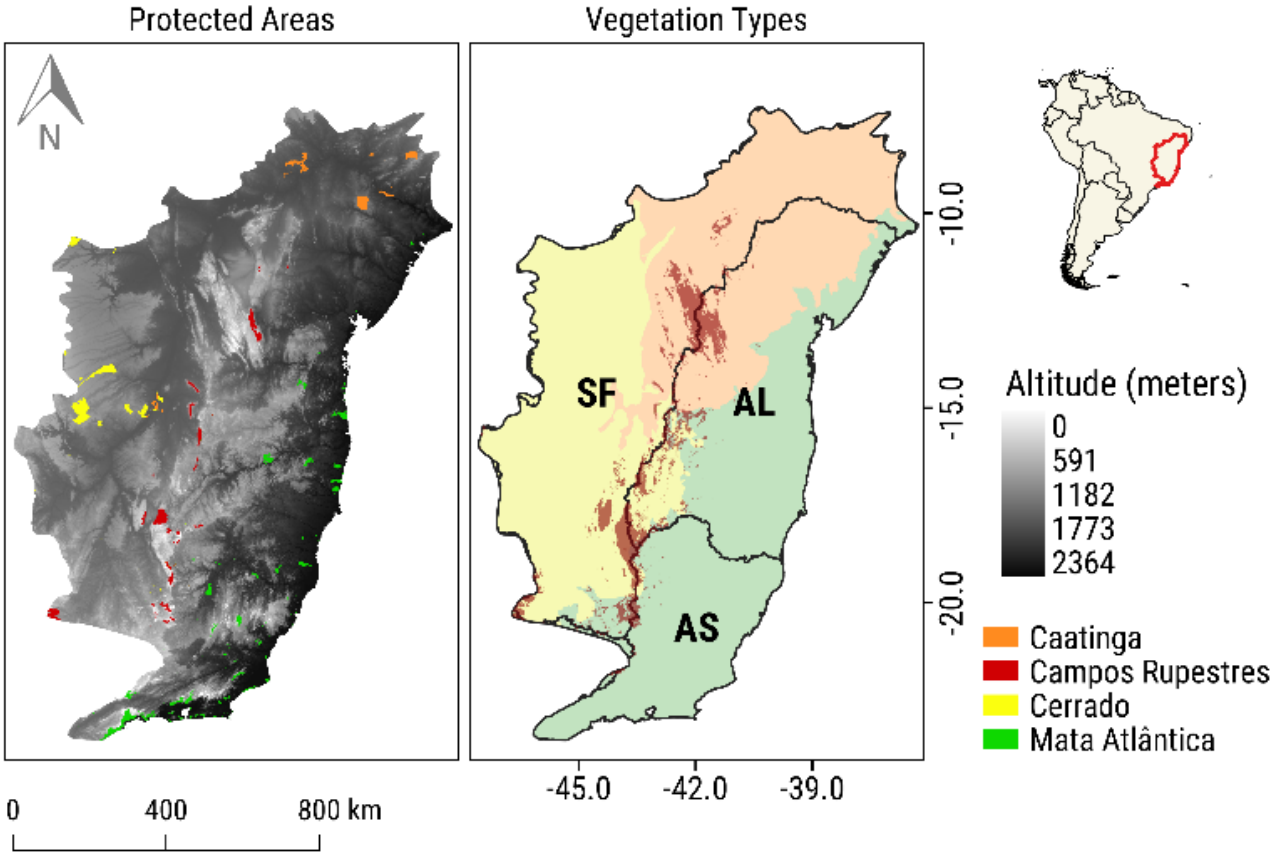

Figure 1. Overview of the Espinhaço mountain range in Brazil. On the left panel, the topography and extent of the Espinhaço Mountain Range and the protected areas classified by vegetation types, in Brazil. On the right, the Espinhaço Range as an ecotone of vegetation types, and as the watershed of São Francisco (SF), Atlântico Leste (AL) and Atlântico Sudeste (AS) basins.

3. RESULTS

The pixel-wise linear regression between NDVI and either precipitation or CWD showed an inverse vegetation response to hydroclimatic variables (Figure 2). We found a general spatial pattern of higher responses of NDVI to CWD for monthly pairwise linear regressions, while the highest explained variance for precipitation was found using a 2-month lagged regression (Figure 2 A and 2 C).

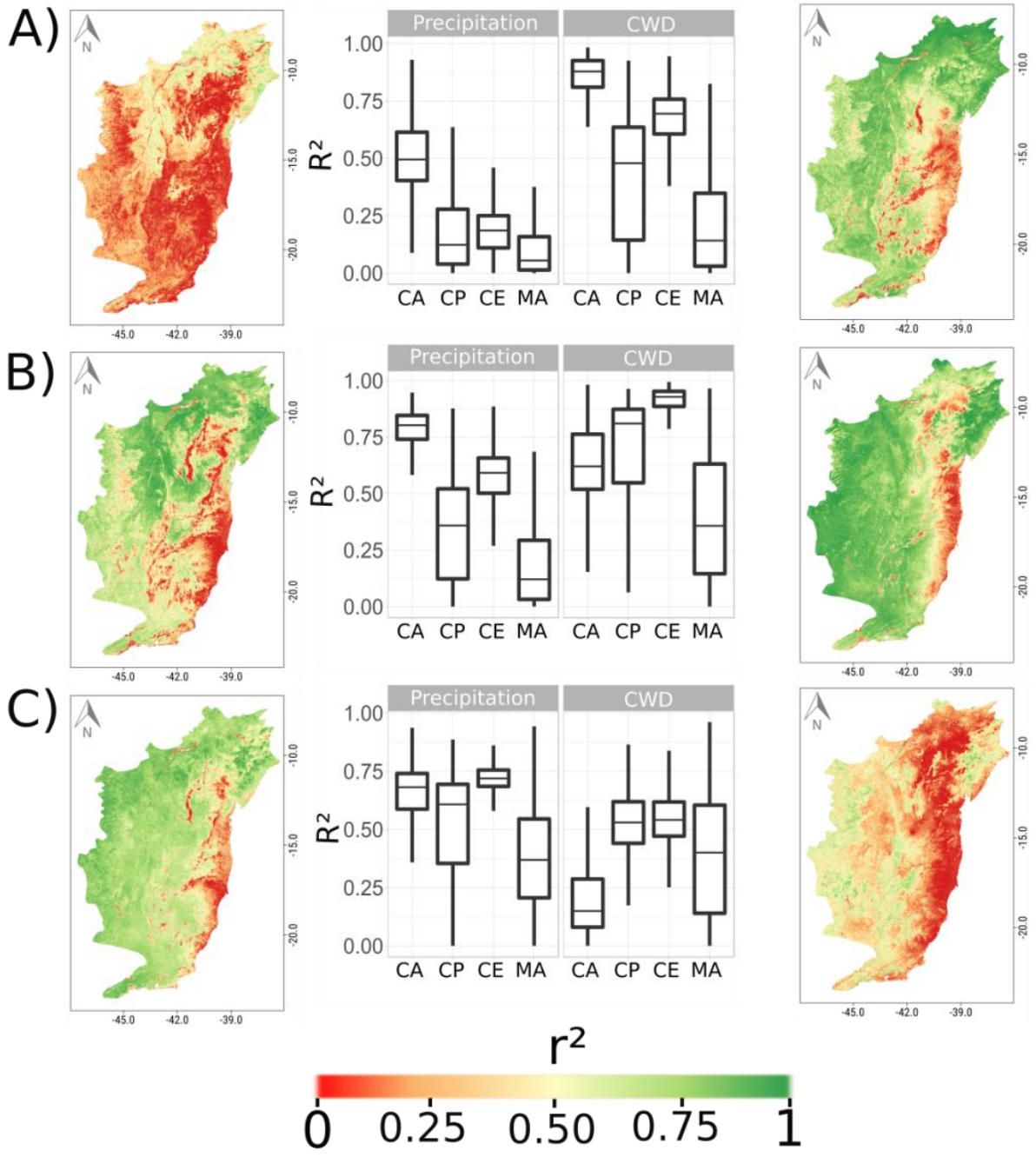

Figure 2. A) Pairwise linear regression; B) 1-month lag linear regression; C) 2-month lag linear regression. Maps resulted from the linear regression between NDVI (Jan/2001 to Dec/2017) and CHIRPS precipitation dataset (Jan/2001 to Dec/2017) (A; B and C left panels) and Climatic Water Deficit (Jan/2001 to Dec/2017) (A; B and C right panels), and boxplots of the r² resulted from the linear regressions (A; B and C middle panels) for each vegetation type sampled at known protected areas (CA = Caatinga; CP = Campos Rupestres; CE = Cerrado; MA = Mata Atlântica)

"Caatinga" vegetation productivity better responded to pairwise CWD (median $r^2 = 0.87$) and had the worst results when using 2-month lag CWD (median $r^2 = 0.14$). "Campos Rupestres" was most responsive to 1-month lag CWD (median $r^2 = 0.80$) and least to 0-lag pairwise precipitation (median $r^2 = 0.12$). "Cerrado" productivity was better explained by 1-month lag CWD (median $r^2 = 0.92$) and had the lowest responses to pairwise precipitation (median $r^2 = 0.18$). "Mata Atlântica" productivity was the least responsive to hydroclimatic variables among all vegetation types, with its largest amount of variance explained by 2-month lag CWD (median $r^2 = 0.40$) and the smallest by the pairwise precipitation regression (median $r^2 = 0.05$).

4. DISCUSSION

The amount of water available to plants is a result of the balance between hydrological inputs and outputs controlled by the amount of energy held in a system. Our results show that the most commonly used variable in ecological predictive models, precipitation, oversimplifies this hydroclimatic aspect, since vegetation productivity responses were poorly correlated to pairwise rainfall. Vegetation responses to CWD, a variable that accounts for the simultaneous availability of water and energy usable by plants, better explained NDVI variation in almost all cases.

"Caatinga" vegetation, which experiences seasonally dry to dry environments, was highly correlated with almost every hydroclimatic variable, with the exception of pairwise precipitation and 2-month lag CWD. Caatinga vegetation productivity is highly dependent on water, shedding their leaves to escape from drought, with the majority of plants presenting this drought avoidance strategy to periods of low water availability (Colwell *et al.*, 2008; Streher *et al.*, 2017). The dry season experienced by caatinga is characterized by a long period of low to the absence of rainfall together with extremely

high temperatures, that is, an excess of energy availability. Thus, the 1-month lag of precipitation explaining a greater variance on NDVI for this vegetation type, indicates that water takes around 1-month after the rainfall event to be available to plant use. This is a result of the first rainfall events in the beginning of the rainy season being rapidly evaporated to attend the high atmospheric evaporative demand from the dry season. However, caatinga vegetation is highly tuned to CWD, given the capacity of this variable to capture the coupling between small variations on water inputs and vegetation productivity, expressed by this balance between water inputs and atmospheric evaporative demand.

"Campos Rupestres" are found on mountaintops, associated with high topographic variation and rugged relief (Silveira *et al.*, 2016). Runoff accounts for a major portion of the water balance in these environmental conditions, justifying the higher explained variance between vegetation productivity and the timing of precipitation. In addition, campos rupestres in high altitudes experience a near-constant presence of cloud cover, and consequently a lower amount of energy coming from solar radiation (Streher *et al.*, 2017). This way, "Campos Rupestres" productivity is better correlated to a 1-month lag CWD, demonstrating that this vegetation demands a certain accumulation of water and energy to be responsive.

The higher r^2 found for "Cerrado" productivity between 1-month lag CWD and 2-month lag precipitation is a function of the relations between topoedaphic conditions and energy availability. The "*Cerrado*" distribution is related to a region with high water retaining capacity, but the high irradiance and elevated temperatures during the dry season deplete the upper soil layers of water in this period (Quesada *et al.*, 2008). Given the smooth topography and well-drained soils, deep-rooted plants can access water from the deeper soil layers even during the dry season, explaining the largest portion of productivity

variance explained by the 2-month lag precipitation response. However, the best response was still found for the 1-month lag CWD, when there is a better balance between rainfall inputs and energy availability, especially during the rainy season.

The moist vegetation typical of the "Mata Atlântica" biome showed the lowest response between plant productivity and hydroclimatic variables, as a result of high-water availability throughout the year. This suggests that water availability may not be the main driver of vegetation productivity, in relation to other environmental conditions. Tropical moist forest phenology is usually characterized by continuous leaf flushing, as shown for Mata Atlântica (Morellato *et al.*, 2000) and Amazonia (Lopes *et al.*, 2016), with high influence of irradiance and cloud cover (Morellato *et al.*, 2000; Streher *et al.*, 2017).

5. CONCLUSIONS

The vegetation types analyzed across the study area, with exception of "Mata Atlântica", were highly correlated with hydroclimatic variables, especially with CWD, with variations in the timing of response regarding its experienced environmental conditions. We conclude that CWD is a better hydroclimatic predictive variable when analyzing vegetation dynamics in dry to seasonally dry regions, since it has the ability to capture plant response patterns to the amount of energy and water, in the spatial and temporal dimensions.

6. REFERENCES

2. Mod, H. K., Scherrer, D., Luoto, M., Guisan, A., & Scheiner, S. (2016). What we use is not what we know: environmental predictors in plant distribution models. *Journal of Vegetation Science*

3. Hawkins, B. A., Field, R., Cornell, H. V., Currie, D. J., Guégan, J.-F., Kaufman, D. M., … Turner, J. R. G. (2003). Energy, water, and broad-scale geographic patterns of species richness. *Ecology*

4. Stephenson, N. (1998). Actual evapotranspiration and deficit: biologically meaningful

correlates of vegetation distribution across spatial scales. *Journal of Biogeography*

5. Dilts, T. E., Weisberg, P. J., Dencker, C. M., & Chambers, J. C. (2015). Functionally relevant climate variables for arid lands: a climatic water deficit approach for modelling desert shrub distributions. *Journal of Biogeography*

6. Allen, K. et. al (2017). Will seasonally dry tropical forests be sensitive or resistant to future changes in rainfall regimes? *Environmental Research Letters*

7. Aparecido, L. M. T., Teodoro, G. S., Mosquera, G., Brum, M., Barros, F. de V., Pompeu, P. V., … Oliveira, R. S. (2018). Ecohydrological drivers of Neotropical vegetation in montane ecosystems. *Ecohydrology*

8. Allan, R. P., & Soden, B. J. (2008). Atmospheric Warming and the Amplification of Precipitation Extremes. *Science*

9. Schaefer, C. E. *et al.* (2016). The Physical Environment of Rupestrian Grasslands (Campos Rupestres) in Brazil: Geological, Geomorphological and Pedological Characteristics, and Interplays. In *Ecology and Conservation of Mountaintop grasslands in Brazil*. Springer International Publishing.

10. Streher, A. S., Sobreiro, J. F. F., Morellato, L. P. C., & Silva, T. S. F. (2017). Land Surface Phenology in the Tropics: The Role of Climate and Topography in a Snow-Free Mountain. *Ecosystems*

11. Busetto, L., & Ranghetti, L. (2016). MODIStsp: An R package for automatic preprocessing of MODIS Land Products time series. *Computers and Geosciences*

12. Funk, C., et al. (2015). The climate hazards infrared precipitation with stations—a new environmental record for monitoring extremes

13. Abatzoglou, J. T., Dobrowski, S. Z., Parks, S. A., & Hegewisch, K. C. (2018). TerraClimate, a high-resolution global dataset of monthly climate and climatic water balance from 1958–2015. *Scientific Data*

14. Colwell, R. K., Brehm, G., Cardelus, C. L., Gilman, A. C., & Longino, J. T. (2008). Global Warming, Elevational Range Shifts, and Lowland Biotic Attrition in the Wet Tropics. *Science*

15. Silveira, F. A. O. et. al(2016). Ecology and evolution of plant diversity in the endangered campo rupestre: a neglected conservation priority. *Plant and Soil*

16. Quesada, C. A., Hodnett, M. G., Breyer, L. M., Santos, A. J. B., Andrade, S., Miranda, H. S., … Lloyd, J. (2008). Seasonal variations in soil water in two woodland savannas of central Brazil with different fire histories. *Tree Physiology*

17. Morellato, L. P. C., Talora, D. C., Takahasi, A., Bencke, C. C., Romera, E. C., & Zipparro, V. B. (2000). Phenology of Atlantic Rain Forest Trees: A Comparative Study1. *Biotropica*

18. Lopes, A. P. et al. (2016). Leaf flush drives dry season green-up of the Central Amazon. *Remote Sensing of Environment*